Testing for Jumps in a Discretely Observed Price Process with Endogenous Sampling Times*

Qiyuan Li† Yifan Li‡ Ingmar Nolte§ Sandra Nolte¶ Shifan Yu‖

This Version: July 20, 2024

Abstract

This paper introduces a novel nonparametric high-frequency jump test for discretely observed Itô semimartingales. Based on observations sampled recursively at first exit times from a symmetric double barrier, our method distinguishes between threshold exceedances caused by the Brownian component and jumps, which enables the construction of a feasible, noise-robust statistical test. Simulation results demonstrate superior finite-sample performance of our test compared to classical methods. An empirical analysis of NYSE-traded stocks provides clear statistical evidence for jumps, with the results highly robust to spurious detections.

JEL Classifications: C12, C14, C22, C58

Keywords: High-Frequency Data, Jump Test, Market Microstructure Noise, Stochastic Sampling Scheme, First Exit Time

*We thank the Co-Editor Torben G. Andersen, the Associate Editor, and two anonymous referees for their insightful comments and suggestions, which greatly improved the quality of this paper. We also thank Leopoldo Catania (discussant), Carsten Chong, Kim Christensen, Dobrislav Dobrev, Roxana Halbleib, Seok Young Hong, Aleksey Kolokolov, Sébastien Laurent, Manh Pham, Roberto Renò, George Tauchen, Stephen Taylor, Viktor Todorov, Giovanni Urga, as well as participants at the CFE-CMStatistics 2020, 6th KoLaMaFr Workshop on Financial Econometrics, XXIII Workshop on Quantitative Finance, Conference on Intrinsic Time in Finance, Economics of Financial Technology Conference 2022, EcoSta 2022, QFFE 2022, IAAE 2022, Econometric Society Asian Meeting 2022, SoFiE 2022, AsianFA 2022, Workshop on Volatility, Jumps and Bursts, Econometric Society Australasian Meeting 2022, 25th Dynamic Econometrics Conference, and seminars at various institutions, for helpful comments and suggestions. Shifan Yu acknowledges financial support from the Economic and Social Research Council (ESRC) North West Social Science Doctoral Training Partnership (ES/P000665/1). The usual disclaimer applies.

†School of Economics, Singapore Management University, 90 Stamford Road, Singapore 178903. Email: qyli.2019@phdecons.smu.edu.sg.

‡Alliance Manchester Business School, University of Manchester, Booth Street West, Manchester M15 6PB, United Kingdom. Email: yifan.li@manchester.ac.uk.

§Lancaster University Management School, Lancaster LA1 4YX, United Kingdom. Email: i.nolte@lancaster.ac.uk.

¶Lancaster University Management School, Lancaster LA1 4YX, United Kingdom. Email: s.nolte@lancaster.ac.uk.

‖Corresponding author, Lancaster University Management School, Lancaster LA1 4YX, United Kingdom. Email: s.yu7@lancaster.ac.uk.

1 Introduction

There exists a consensus in the financial literature that modelling asset price dynamics requires the specification of different components. In addition to the stochastic volatility component which accommodates the persistence of volatility, "jumps" in asset prices serve as an explanation for abnormal large variations which play an important role in the tail behavior of return distributions. Jumps are believed to contain predictive information so that the correct identification of jumps usually leads to improved price or volatility forecasts and portfolio outcomes (see, e.g., Yan, 2011, Jiang and Yao, 2013, Cremers et al., 2015, for empirical applications using daily or monthly financial data, and Andersen et al., 2007a, Corsi et al., 2010, Nolte and Xu, 2015, Bollerslev et al., 2015, 2020, Pelger, 2020, for those using high-frequency intraday data). The increased availability of high-frequency financial data has further motivated the development of methodologies designed to test the model specification based on a discretely observed semimartingale.

Over the past two decades, a number of nonparametric jump tests have been developed. Starting from the seminal work of Barndorff-Nielsen and Shephard (2004), most of these tests are constructed on jump-robust measures of returns or their variations, see, e.g., Huang and Tauchen (2005), Barndorff-Nielsen and Shephard (2006), Andersen et al. (2007b), Jiang and Oomen (2008), Lee and Mykland (2008), Aït-Sahalia and Jacod (2009), Corsi et al. (2010), Podolskij and Ziggel (2010), Andersen et al. (2012), Lee and Mykland (2012), and Aït-Sahalia et al. (2012), among others. Some recent works focus on modified versions of these tests when conventional assumptions are violated, see, e.g., Laurent and Shi (2020) and Kolokolov and Renò (2024), and tests for co-jumps in a collection of assets, see, e.g, Bibinger and Winkelmann (2015) and Caporin et al. (2017).

Despite the theoretical developments in the literature, these jump tests in practice can sometimes deliver inconsistent results. Theodosiou and Žikeš (2011), Dumitru and Urga (2012), and Maneesoonthorn et al. (2020) conduct comparisons of various tests based on Monte Carlo simulations and real-world high-frequency data. These papers convincingly show that the performances of various jump tests depend crucially on: (i) the choice of sampling interval, and (ii) the assumption about market microstructure noise. For the first issue, a large sampling interval is typically needed for most classical tests to alleviate the impact of noise, but it also has a detrimental effect on their statistical power. As a result, it is difficult to determine an appropriate sampling interval for these tests in practice. For the second issue, Dumitru and Urga (2012) illustrate that ignoring even an independent and identically distributed (i.i.d.) additive noise can result in significant size distortion for the "star performers" in the literature. It is obvious that a more intricate noise specification, such as those discussed in Kalnina and Linton (2008), Bandi and Russell (2008), Aït-Sahalia et al. (2011), Hautsch and Podolskij (2013), Jacod et al. (2017), Li et al. (2020), Da and Xiu (2021), and Li and Linton (2022), can further muddle this issue.

In this paper, we introduce an innovative nonparametric method to test for jumps in a discretely observed semimartingale. Different from the conventional practice of sampling observations at equidistant intervals in calendar time, our methodology adopts a path-dependent approach to sample

tick-by-tick observations, inspired by the works of Engle and Russell (1998), Andersen et al. (2008), Fukasawa and Rosenbaum (2012), Vetter and Zwingmann (2017), and Hong et al. (2023): Sampling times are recursively determined by the first exit time of price movements from a symmetric barrier since the previous sampled observation. This endogenous sampling scheme is tailored to be sensitive to discontinuities. Specifically, jumps of sizes larger than the barrier width will immediately trigger the stopping rule and induce large "overshoots" or threshold exceedances. To distinguish between threshold exceedances caused by discrete Brownian steps and those by jumps, we censor the returns between consecutive sampling times with a specific threshold,[1] and construct a standardized test statistic to measure the potential distortion caused by disproportionately large overshoots on the sample moment of returns. Furthermore, we develop a two-step noise reduction method inspired by the pre-averaging approach of Jacod et al. (2009) and the wild bootstrap introduced by Wu (1986) to mitigate the impact of weakly dependent market microstructure noise.

Simulation results reveal that our new high-frequency jump test exhibits reliable finite-sample size and power performance across various aggregation levels, and its performance is robust to measurement errors simulated with a realistically calibrated specification. A comparison with traditional tests constructed from equidistantly sampled observations and some noise-robust versions based on ultra-high-frequency data is conducted thereafter. We find that (i) most calendar-time-sampled tests exhibit less consistent performance across different sampling frequencies and are poorly sized in the presence of noise, which is in line with the Monte Carlo results of Dumitru and Urga (2012) and Maneesoonthorn et al. (2020), and (ii) while noise-robust tests maintain reliable sizes, their power performance still lags behind our test across a wide range of simulation settings. In an empirical application, our test is applied to transaction data of 10 selected stocks listed on the New York Stock Exchange (NYSE). Clear statistical evidence of jumps is found for all selected stocks, with jumps occurring on approximately 10% to 15% of trading days. Furthermore, the test rejections are highly robust to the correction of spurious detections based on the method of Bajgrowicz et al. (2016).

The remainder of this paper is structured as follows: Section 2 lays out the basic setup and key assumptions. Section 3 discusses the test statistic and its asymptotic theory, along with the noise reduction technique. Section 4 assesses the finite-sample performance of our new test with Monte Carlo simulations. After discussing the empirical application for selected NYSE stocks in Section 5, we conclude in Section 6. All proofs and additional materials are relegated to the Appendix.

[1] Related works about the boundary crossing problems for random walks, especially those with Gaussian steps, include Rogozin (1964), Lorden (1970), Lotov (1996), and Khaniyev and Kucuk (2004). The idea of censored increments in this paper was inspired by the truncated realized volatility of Mancini (2009), which is the first work that utilizes the systematic observation error as an effective way to eliminate the impact of jumps.

2 Setting and Assumptions

We consider a one-dimensional underlying process $X = (X_t)_{t\geq 0}$ for the efficient logarithmic price of a financial asset. We assume that X follows a possibly discontinuous Itô semimartingale defined on a filtered probability space $(\Omega, \mathcal{F}, (\mathcal{F}_t)_{t\geq 0}, \mathbb{P})$:

$$\begin{aligned} X &= X' + X'', \\ X'_t &= X_0 + \int_0^t \mu_s ds + \int_0^t \sigma_s dW_s, \\ X''_t &= \int_0^t \int_{|\delta|\geq u} \delta(s,x) \underline{p}(ds,dx), \end{aligned} \tag{1}$$

where t stands for time, W is a standard Brownian motion, $\underline{p}(dt,dx)$ is a Poisson random measure on $\mathbb{R}_+ \times \mathbb{R}$ with a compensator $\underline{q}(dt,dx) = dt \otimes \lambda(dx)$, and λ is a σ-finite measure on $\mathbb{R}_+$. We assume that X satisfies the following regularity conditions:

Assumption 1. (i) The process μ is optional and locally bounded;
(ii) The process σ is càdlàg (i.e., right-continuous with left limits), adapted, and strictly positive;
(iii) There exists a sequence $(\tau_m)_{m\geq 1}$ of stopping times increasing to ∞, and a sequence $(K_m)_{m\geq 1}$ of finite constants, such that it holds for each $m \geq 1$ that $\mathbb{E}[|\sigma_{t\wedge\tau_m} - \sigma_{s\wedge\tau_m}|^2] \leq K_m|t-s|$ for all $s,t \in [0,T]$ with some finite T;
(iv) The function $\delta(\omega,t,x)$ on $\Omega \times \mathbb{R}_+ \times \mathbb{R}$ is predictable;
(v) There is a localizing sequence $(\tau_n)_{n\geq 1}$ of stopping times increasing to ∞, and a sequence $(f_n)_{n\geq 1}$ of deterministic nonnegative functions on $\mathbb{R}$, which satisfies $|\delta(\omega,t,x)| \wedge 1 \leq f_n(x)$ for all (ω,t,x) with $t \leq \tau_n(\omega)$, and $\int_{\mathbb{R}} |f_n|^r \lambda(dx) < \infty$ for some $r \in [0,1)$.

Remark 1. Assumption 1 entails some very mild technical conditions that the coefficients in Eq. (1) should meet. Condition (iii) states that the spot volatility process is locally 1/2-Hölder continuous under the L_2-norm. The smoothness condition is satisfied whenever σ is an Itô semimartingale, or a long-memory process driven by a fractional Brownian motion (Bollerslev et al., 2021). The parameter r in Condition (v) sets a bound on the degree of jump activity, which can be interpreted as a generalized version of the Blumenthal-Getoor index for a Lévy process. With some $r \in [0,1)$, we consider jumps of both finite and infinite activities, but restrict them to be of finite variation, i.e., they are absolutely summable, such that in Eq. (1) we dispense with the integral with $\underline{p} - \underline{q}$, see Jacod et al. (2019) for more details.

Remark 2. For the pure jump process X'' in Eq. (1), integrating $\delta(s,x)$ over the range $(-\infty,-u] \cup [u,\infty)$ for some $u > 0$ removes all jumps of sizes smaller than u. For any fixed u, X'' is a finite-activity jump process. As $u \to 0$, X'' retains both "big" and "small" jumps, such that it converges pathwise to a process of infinite-activity jumps with finite variation. As only discrete observations of the realized sample path $X(\omega)$ are available, we shall assume a slightly higher order in probability for u compared to X' as the number of observations increases, which excludes the very small jumps

relative to the increments of X'. Further clarification will be provided in Section 2.1 after detailing our observation scheme.

The quadratic variation (QV) of X over a finite interval $[0,t]$ is defined as

$$[X,X]_t = \int_0^t \sigma_s^2 ds + \sum_{0\le s\le t} (\Delta X_s)^2, \quad \text{with } \Delta X_t = X_t - X_{t-}, \tag{2}$$

where the integrated variance (IV), $\int_0^t \sigma_s^2 ds$, summarizes the variation from X'.

Testing for jumps is a procedure to answer the fundamental question of whether the realized sample path $X(\omega)$ is continuous or not over a finite time interval, e.g., $(0,1)$.[2] Technically speaking, we decompose the sample space Ω into two complementary subsets:

$$\begin{aligned} \Omega' &= \left\{\omega : X_t''(\omega) = 0,\ \forall t \in (0,1)\right\}, \\ \Omega'' &= \left\{\omega : X_t''(\omega) \neq 0,\ \exists t \in (0,1)\right\}, \end{aligned} \tag{3}$$

where Ω' (resp. Ω'') represents the null hypothesis (alternative hypothesis) for a jump test, which assesses the plausibility of these two hypotheses based on discrete observations of $X(\omega)$.

2.1 Observation Scheme

We now describe how observations take place.[3] At stage n, we assume that the successive observations of $X(\omega)$ occur at times $0 = t_{n,0} < t_{n,1} < \dots$ for a sequence $(t_{n,i})$ of discrete times over a fixed interval (such as a trading day), which is normalized to the unit interval $[0,1]$. We set

$$N_t^n = \sum_{i\ge 1} \mathbb{1}_{\{t_{n,i}\le t\}} \qquad \text{and} \qquad \Delta_{n,i} = t_{n,i} - t_{n,i-1}, \tag{4}$$

where $N \equiv N_1^n$ stands for the number of observations on $(0,1]$, and $\Delta_{n,i}$ is the i-th inter-observation lag at stage n. It is easily seen from the empirical tick-level data that the observation times are far from evenly spaced and usually dependent on $X(\omega)$ itself. Our assumption for the observation scheme over $[0,1]$ is outlined as follows:

Assumption 2. Let Δ_n be a positive sequence of real numbers satisfying $\Delta_n \to 0$ as $n \to \infty$. We define an intensity process of observations $\lambda = (\lambda_t)_{0\le t\le 1}$ with $\lambda_t = K\sigma_t^2$ for some $K > 0$. There exists a localizing sequence $(\tau_m)_{m\ge 1}$ of stopping times and positive constants $K_{m,p}$ and κ such that:

(i) With $(\mathcal{F}_t^n)_{t\ge 0}$ the smallest filtration containing $(\mathcal{F}_t)_{t\ge 0}$ and with respect to which all observation times $t_{n,i}$ are stopping times, for each $i = 1,2,\dots$, the variable $\Delta_{n,i}$ is, conditionally on

[2] We restrict the alternative hypothesis to contain at least one jump on $(0,1)$ as it is not feasible for a test to identify jumps occurring right at both end-points of the interval.

[3] We would like to distinguish the terms "observation scheme" and "sampling scheme" in this paper. We allow both tick-level and sampled observations to form discrete-time processes, and the term "sampling" refers to a subsampling or subset selection procedure for the discrete observations at the highest frequency.

$\mathcal{F}^n_{i-1} \equiv \mathcal{F}^n_{t_{n,i-1}}$, independent of $\mathcal{F}_\infty = \bigvee_{t\geq 0} \mathcal{F}_t$.

(ii) With the restriction $\{t_{i-1} < \tau_m\}$, we have for all $p \geq 2$,

$$\begin{aligned} \mathbb{E}[|\Delta_{n,i}\lambda_{t_{n,i-1}} - \Delta_n||\mathcal{F}^n_{i-1}] &\leq K_{m,1}\Delta_n^{2+\kappa}, \\ \mathbb{E}[|\Delta_{n,i}\lambda_{t_{n,i-1}}|^p|\mathcal{F}^n_{i-1}] &\leq K_{m,p}\Delta_n^p. \end{aligned} \tag{5}$$

A useful consequence of this Assumption is the following convergence in probability:

$$\Delta_n N^n_t \xrightarrow{\mathbb{P}} \tau(t) = \int_0^t \sigma_s^2 ds. \tag{6}$$

Remark 3. Assumption 2 is inspired by Assumption (O) of Jacod et al. (2017) and Assumption (O-ρ, ρ') of Jacod et al. (2019). The process λ controls for the "spot" observation arrival rates, and the unobserved Δ_n can be interpreted as an "average mesh size" between successive observations. Our choice of the intensity $\lambda = K\sigma^2$ implies higher observation frequencies of $X(\omega)$ during periods of high local volatility, which captures the diurnal patterns of transaction activities and intraday volatility. This is motivated by the empirical evidence of the E-mini S&P 500 futures contract in Andersen et al. (2018), which illustrates a notable similarity in the intraday U-shaped patterns of one-minute transaction counts and return variation, where the pronounced spikes, typically align with market openings or announcements, roughly coincide. Note that λ is defined up to scale, which allows $K = 1$ to be set without loss of generality (by scaling Δ_n correspondingly), as further discussed in Jacod et al. (2017).

Remark 4. With the convergence result in Eq. (6), Assumption 2 implies a time-changed regular observation scheme under infill asymptotics: As $n \to \infty$, the observation time $t_{n,i}$ converges to $\breve{t}_{n,i} = \inf\{t \in [0,1] : \tau(t) = i\Delta_n\}$. This limiting observation scheme corresponds to Example 2.2 in Jacod et al. (2017). In contrast to the calendar time t, the "intrinsic time" $\tau(t)$ evolves endogenously with respect to the variation from X'. The time change induces a certain level of endogeneity, and extends the commonly assumed equidistant observation scheme in high-frequency financial econometrics literature (Li et al., 2014; Dimitriadis and Halbleib, 2022; Dimitriadis et al., 2023). With the irregular mesh sizes $\Delta_{n,i}$ regulated by Condition (ii), the deviation of $(t_{n,i})$ from $(\breve{t}_{n,i})$ vanishes as $n \to \infty$, and has no impact on the limit theorems derived in the next section. Further discussion on this matter can be found in Remark 7 and Appendix A.1.

We now revisit the Itô semimartingale in Eq. (1): Under the assumed observation scheme, we consider a sequence of processes defined on the same probability space $(\Omega, \mathcal{F}, (\mathcal{F}_t)_{t\geq 0}, \mathbb{P})$:

$$X^n_t = X'_t + \int_0^t \int_{|\delta|\geq u_n} \delta(s,x)\underline{p}(ds,dx), \tag{7}$$

and we choose a sequence u_n of real numbers satisfying

$$\frac{u_n}{\sqrt{\Delta_n}} \to \infty \qquad \text{and} \qquad u_n\Delta_n^{\beta-1/2} \to 0, \tag{8}$$

for any $0 < \beta \leq 1/2$. The choice of u_n of a slightly higher order than $\sqrt{\Delta_n}$ guarantees that, as $n \to \infty$, the integral with Poisson measure $\underline{p}$ in Eq. (7) retains both "big" and "small" jumps but excludes the very small ones of order $O_p(\sqrt{\Delta_n})$, i.e., the local alternative in the literature (see Remark 10.27, Aït-Sahalia and Jacod, 2014). Our test is designed to identify the existence of both the finite-activity and local-to-infinite-activity jumps which dominate the increments of X'.

2.2 Price Duration Sampling

Sparse sampling is widely adopted in both the financial econometrics literature and by practitioners to mitigate the impact of market microstructure noise, with some popular choices like 1-minute and 5-minute sampling in calendar time (Aït-Sahalia et al., 2005; Liu et al., 2015). However, such sparse sampling aggregates a substantial amount of tick-level returns exogenously, which dilutes the relative size of jumps and inevitably reduces the power of jump tests. This phenomenon is evident in the Monte Carlo results of Dumitru and Urga (2012) and Maneesoonthorn et al. (2020): Nearly all traditional tests constructed from calendar-time-sampled returns exhibit rapid power loss as sampling becomes sparser.[4]

In response to this issue, a path-dependent sampling scheme seems a natural solution. We consider a stochastic and endogenous sampling scheme for all observations of $X(\omega)$ on $[0,1]$: Let $(X_i)_{0\leq i\leq N}$ collect all observations under Assumption 2. With a selected barrier width $c > 0$, the price duration sampling (PDS) is defined as the following sampling algorithm:

1. Set $\Pi_0^{(c)} = 0$.
2. For $j = 1, 2, \ldots,$ sample X_i for all $i = \Pi_j^{(c)}$ that are decided recursively by

$$\Pi_j^{(c)} = \inf\left\{\Pi_{j-1}^{(c)} < i \leq N : \left|X_i - X_{\Pi_{j-1}^{(c)}}\right| \geq c\right\}. \tag{9}$$

We therefore obtain a subsequence $X^{(c)} = (X_{\Pi_j^{(c)}})_{0\leq j\leq N^{(c)}}$, where $N^{(c)} = \max_{j\geq 1}\{\Pi_j^{(c)} \leq N\}$ counts the total number of sampled observations. Moreover, we define the PDS returns as the increments of $X^{(c)}$, i.e., $r_j^{(c)} = X_{\Pi_j^{(c)}} - X_{\Pi_{j-1}^{(c)}}$ for all $j \in \{1, 2, \ldots, N^{(c)}\}$.

Remark 5. The above sampling algorithm is a discrete-time version of PDS in Hong et al. (2023). The idea of sampling financial observations based on hitting or exit times was initially proposed by Engle and Russell (1998), and has been further developed since then (Gerhard and Hautsch, 2002; Andersen et al., 2008; Tse and Yang, 2012; Fukasawa and Rosenbaum, 2012; Vetter and Zwingmann, 2017; Hong et al., 2023). While previous studies have primarily focused on volatility estimation based on this alternative sampling scheme, our contribution stands out as the first to demonstrate that this scheme can be exploited to construct more effective high-frequency jump tests.

[4]Some noise-robust tests constructed from filtered data, such as those proposed by Lee and Mykland (2012) and Aït-Sahalia et al. (2012), can utilize all available observations without sampling. As alternative methods that exploit data more sufficiently than classical approaches, we compare their finite-sample performance with our method through simulations in Section 4.

This endogenous sampling scheme is designed to be highly sensitive to the presence of jumps. Fig. 1 demonstrates some examples when $X(\omega)$ is continuous and discontinuous, respectively. When $X(\omega)$ is continuous, each sampled return under PDS ("PDS return", i.e., first ladder height with respect to c) consists of the barrier width c and a small threshold exceedance attributed to the discreteness of price observations. When $X(\omega)$ is discontinuous, any single jump larger than c will always trigger an exit-time event in Eq. (9), and induce a large "overshoot".

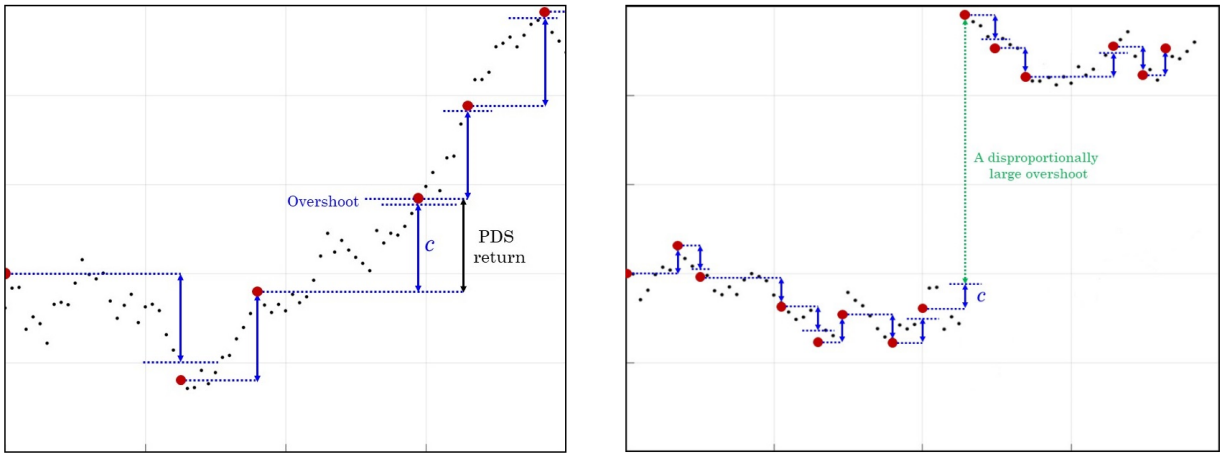

Figure 1: Examples of PDS when $X(\omega)$ is continuous and discontinuous, respectively. Jumps will almost surely lead to the sampling of next available observation, and induce a large overshoot.

The discrepancy between threshold exceedances induced by continuous price increments and jumps can be exploited to construct more powerful jump tests. We provide some preliminary evidence for the impact of different sampling schemes on the power of jump tests with a simple Monte Carlo experiment for an idealized test: We simulate a standard Gaussian random walk with a fixed number of i.i.d. increments (corresponding to the limiting observation scheme in Remark 4), and a fixed-size jump is randomly inserted into each simulated path. We then obtain sampled returns with both PDS and equidistant sampling across a wide range of sampling frequencies. For any (PDS or equidistantly) sampled return, we reject the null hypothesis of no jump if the absolute return exceeds its theoretical 95% quantile under the null. This test maintains the correct size by construction for any sampling frequency. When a fixed-size jump is randomly inserted, the sampling frequency inversely controls the "signal-to-noise" ratio, as the jump size gets diluted by the size of aggregated returns over that interval. This allows us to effectively compare the local power performance of the test under the two sampling schemes.

Fig. 2 reports the power curves of the test under both sampling schemes (under the alternative hypothesis that the tested interval contains a jump). We observe that both curves decay towards the nominal level of 5% as the sampling becomes more sparse. However, the test based on PDS returns exhibits uniformly better power than the one based on equidistantly sampled returns across all common sampling frequencies. Intuitively, this power gain is attributed to the sensitivity of our

sampling algorithm to jumps, which ensures the jump size information is effectively preserved in the threshold exceedance. By contrast, the equidistant sampling scheme aggregates returns exogenously, where the jump size is diluted much more quickly by the decreasing sampling frequency relative to the PDS case. This advantageous property of PDS contributes to a diminished probability of committing a Type II error, and thereby serves as the main motivation for the new statistical test proposed in the next section.

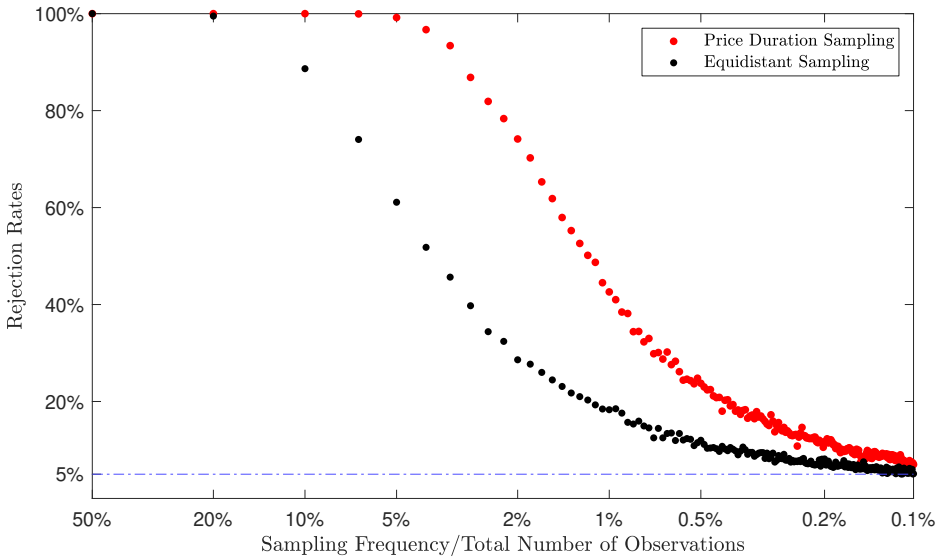

Figure 2: Rejection rates under two different sampling schemes. We simulate 2000 random walk paths with 10^6 standard normal steps (null). A jump of fixed size 10 are randomly inserted in each path. Under two different sampling schemes, the absolute returns containing jumps are compared with the 95% quantiles of absolute sampled returns under the null.

We now formally introduce our asymptotic setting under PDS: We let the barrier width c shrink proportionally to $\sqrt{\Delta_n}$ under infill asymptotics, i.e.,

$$c \equiv c_n = m\sqrt{\Delta_n}, \quad \text{for some constant } m > 0. \tag{10}$$

When $X(\omega)$ is continuous, each absolute PDS return $|r_i^{(c)}|$ is a sum of the barrier width c and a small threshold exceedance caused by the discreteness of observations, which satisfies

$$1 \leq \frac{|r_i^{(c)}|}{c} = O_p(1), \quad \text{for all } i \in \{1, 2, \ldots, N^{(c)}\}. \tag{11}$$

Jumps of a higher asymptotic order than $\sqrt{\Delta_n}$ will almost surely trigger the stopping rule in Eq. (9), and induce some disproportionally large PDS returns with

$$\frac{|r_i^{(c)}|}{c} \xrightarrow{\text{a.s.}} \infty. \tag{12}$$

To distinguish between the "small" overshoots induced by continuous price increments and the "big" overshoots caused by jumps, we censor the (absolute) PDS returns with a threshold $\varphi_\epsilon(c)$ that shrinks to zero at the same rate $\sqrt{\Delta_n}$ as the barrier width c, i.e., for all $i \in \{1, 2, \ldots, N^{(c)}\}$,

$$|\overline{r}_i^{(c)}| = |r_i^{(c)}| \wedge \varphi_\epsilon(c), \quad \text{where } \varphi_\epsilon(c) = c\,(1+\epsilon) \text{ for some constant } \epsilon > 0. \tag{13}$$

Remark 6. The idea of censored returns originates from the truncated realized volatility (TRV) estimator of Mancini (2009), while the fixed choice of ϵ in Eq. (13) is unconventional in the literature. Different from the standard truncation threshold of a slightly higher order than $\sqrt{\Delta_n}$, our selected threshold $\varphi_\epsilon(c) \asymp \sqrt{\Delta_n}$ affects both the increments from X' and X'' under infill asymptotics. This overcomes the "perfect correlation" issue of TRV and RV (Podolskij and Ziggel, 2010), and enables the construction of feasible test statistics that do not necessarily require consistent IV estimation.[5]

3 Main Results

In this section, we introduce and analyze our new test statistic, which is constructed from the PDS returns between sampled observations collected by $X^{(c)}$. Then we augment the test with an effective noise reduction method to mitigate the impact of market microstructure noise.

3.1 Test Statistic

To prepare for the construction of our test statistic, we first introduce the notation for the moments of PDS returns from a standard Gaussian random walk $(Z_i)_{i=0,1,\ldots}$ with a barrier width m, which is denoted as $Z_1^{(m)}$:

(i) Absolute moment of $Z_1^{(m)}$: $\mu_\gamma(m) = \mathbb{E}[|Z_1^{(m)}|^\gamma]$,
(ii) Absolute moment of censored $Z_1^{(m)}$: $\overline{\mu}_{\gamma,\epsilon}(m) = \mathbb{E}[|\overline{Z}_1^{(m)}|^\gamma] = \mathbb{E}[(|Z_1^{(m)}| \wedge \varphi_\epsilon(m))^\gamma]$,
(iii) Absolute cross moment of censored and uncensored $Z_1^{(m)}$: $\overline{\rho}_{\gamma,\epsilon}(m) = \mathbb{E}[|Z_1^{(m)}|^\gamma |\overline{Z}_1^{(m)}|^\gamma]$,

and two first-order differentiable and invertible functions:

$$h_\gamma(m) = \frac{\mu_\gamma(m)}{m^\gamma} \qquad \text{and} \qquad \overline{h}_{\gamma,\epsilon}(m) = \frac{\overline{\mu}_{\gamma,\epsilon}(m)}{m^\gamma}, \tag{14}$$

with the first-order derivatives $h'_\gamma(m)$ and $\overline{h}'_{\gamma,\epsilon}(m)$, and the inverse functions $h_\gamma^{-1}(x)$ and $\overline{h}_{\gamma,\epsilon}^{-1}(x)$.

We will now proceed to define the testing procedures. For all observations $(X_i)_{0\le i\le N}$ under Assumption 2, we obtained the sampled observations in $X^{(c)}$ with the barrier width c that satisfies

[5] With the standard truncation threshold, the realized moments of truncated and untruncated increments have the same asymptotic distribution if $X(\omega)$ is continuous, such that it is impossible to derive the distribution theory for either the linear or ratio test based on the standard TRV and RV estimators. In this paper, as our method does not require consistent IV estimation, we can also adopt the truncation technique of Mancini (2009) and discard all absolute PDS returns that are larger than $\varphi_\epsilon(c)$. However, the censoring approach does not change the total number of PDS returns and is therefore more convenient for both our theoretical derivation and empirical implementation.

Eq. (10). To assess the distortion resulting from "large" overshoots, we compare the sample moments of uncensored and censored PDS returns normalized by the barrier width c, i.e.,

$$S_2 = \frac{1}{N^{(c)}} \sum_{i=1}^{N^{(c)}} \left(\frac{|r_i^{(c)}|}{c} \right)^2 \quad \text{and} \quad \overline{S}_{2,\epsilon} = \frac{1}{N^{(c)}} \sum_{i=1}^{N^{(c)}} \left(\frac{|\overline{r}_i^{(c)}|}{c} \right)^2, \tag{15}$$

with the functions defined in Eq. (14):

$$M_c = h_2^{-1}(S_2) \quad \text{and} \quad \overline{M}_{c,\epsilon} = \overline{h}_{2,\epsilon}^{-1}\left(\overline{S}_{2,\epsilon}\right). \tag{16}$$

Theorem 1 (Consistency)**.** With Assumption 2 satisfied and $c = m\sqrt{\Delta_n}$, it holds that as $n \to \infty$,

$$\begin{aligned} (\overline{M}_{c,\epsilon}, M_c)' &\xrightarrow{\mathbb{P}} (m, m)', \qquad \text{if } \omega \in \Omega', \\ (\overline{M}_{c,\epsilon}, M_c)' &\xrightarrow{\mathbb{P}} (m, m^*)', \qquad \text{if } \omega \in \Omega'', \end{aligned} \tag{17}$$

where $m^* = h_2^{-1}(\kappa \cdot h_2(m))$ with κ the ratio between QV and IV over $[0, 1]$.

Remark 7. The estimators $(\overline{M}_{c,\epsilon}, M_c)'$, constructed from the PDS returns from (i) the observations $(X_i)_{0 \le i \le N}$ on $(t_{n,i})$ with irregular $\Delta_{n,i}$ under Assumption 2, and (ii) the Gaussian random walk formed by observations under the limiting observation scheme $(\breve{t}_{n,i})$ in Remark 4, are shown to have the same limit theorems. These include the law of large numbers (LLN) and the central limit theorem (CLT), both supported by some strong approximation results similarly used in Chernozhukov et al. (2013, 2019), see Appendix A.1 for further details. The consistency and asymptotic distribution in Theorem 1 and the subsequent Theorem 2, respectively, are therefore derived from the random sum LLN and CLT introduced by Anscombe (1952) for randomly indexed random walks (Rényi, 1957; Gut, 2009, 2012). Under the alternative, jumps have no impact on $\overline{M}_{c,\epsilon}$ since $\varphi_\epsilon(c)$ shrinks to zero at the same speed as $\sqrt{\Delta_n}$, while M_c will converge to a different level due to the distortion arising from large overshoots.

Remark 8. Whether $X(\omega)$ is continuous or not, once the barrier width c is chosen, a consistent IV estimator should be proportional to the number of sampled observations $N^{(c)}$. Specifically, with a fully observable sample path $X(\omega)$ over $[0, 1]$, the nonparametric duration-based volatility (NPDV) estimator of Hong et al. (2023), i.e., $\widehat{V} = c^2 N^{(c)}$, is shown to be consistent since all absolute PDS returns are exactly c. In a more realistic setting with an infinite number of discrete observations of $X(\omega)$ over $[0, 1]$, we define $\widehat{V}^* = \tilde{c}^2 N^{(c)}$, where $\tilde{c}^2 = c^2 h_2(\overline{M}_{c,\epsilon})$ is corrected for "small" overshoots from discrete Brownian steps with a consistent estimator of m. Even though the estimation of IV is not the primary focus of this work, it contributes to a more accurate duration-based estimator with the discretization error corrected.

Furthermore, both $\overline{M}_{c,\epsilon}$ and M_c are jointly asymptotically normal under the null with a known variance-covariance matrix, which naturally leads to a well-defined ratio test.

Theorem 2 (Asymptotic normality)**.** Under the same conditions as in Theorem 1, the estimators $\overline{M}_{c,\epsilon}$ and M_c are jointly normally distributed when $\omega \in \Omega'$:

$$\sqrt{N}\begin{bmatrix}\overline{M}_{c,\epsilon}-m\\ M_c-m\end{bmatrix} \xrightarrow{\mathcal{L}} \mathcal{N}\left(\begin{bmatrix}0\\0\end{bmatrix},\begin{bmatrix}\phi_{11} & \bullet\\ \phi_{21} & \phi_{22}\end{bmatrix}\right), \tag{18}$$

where

$$\phi_{11} = \frac{\mu_2(m)(\overline{\mu}_{4,\epsilon}(m)-\overline{\mu}^2_{2,\epsilon}(m))}{m^4(\overline{h}'_{2,\epsilon}(m))^2}, \tag{19}$$

$$\phi_{22} = \frac{\mu_2(m)(\mu_4(m)-\mu_2^2(m))}{m^4(h'_2(m))^2}, \tag{20}$$

$$\phi_{21} = \frac{\mu_2(m)(\overline{\rho}_{2,\epsilon}(m)-\mu_2(m)\overline{\mu}_{2,\epsilon}(m))}{m^4(h'_2(m)\overline{h}'_{2,\epsilon}(m))^2}. \tag{21}$$

Corollary 1. Under the same conditions, the standardized ratio test statistic $T_{c,\epsilon}$ satisfies

$$T_{c,\epsilon} = \frac{\overline{M}_{c,\epsilon}/M_c - 1}{\sqrt{\widehat{V}_\epsilon(\overline{M}_{c,\epsilon})}} \quad \begin{cases} \xrightarrow{\mathcal{L}} \mathcal{N}(0,1) & \text{if } \omega \in \Omega', \\ \xrightarrow{\mathbb{P}} \infty & \text{if } \omega \in \Omega'', \end{cases} \tag{22}$$

where the denominator is the estimated standard deviation of $\overline{M}_{c,\epsilon}/M_c$ with

$$\widehat{V}_\epsilon(m) = \frac{1}{m^2 N}(\phi_{11}+\phi_{22}-2\phi_{21}). \tag{23}$$

When $X''(\omega) \equiv 0$ on the interval $(0,1)$, the test statistic $T_{c,\epsilon}$ converges in distribution to a standard normal random variable, which is implied by Theorem 2. When $X''(\omega) \neq 0$ for some $t \in (0,1)$, the numerator of $T_{c,\epsilon}$ converges to a finite non-zero level determined by κ, whereas its denominator shrinks to zero as $n \to \infty$. Consequently, the standardized test statistic diverges in the limit, thereby implying the consistency of the test under the alternative hypothesis.

3.2 Noise Mitigation

As discussed in Remark 7, our asymptotic results derived in Section 3.1 are based on the conclusion that our estimators constructed from the sampled returns of (i) the observations on $(t_{n,i})$ under Assumption 2, and (ii) the observations on $(\breve{t}_{n,i})$ in Remark 4, have the same limit theorems. Since the observations on $(\breve{t}_{n,i})$ form a random walk with all i.i.d. Gaussian steps, the sampled observations under PDS constitute a stopped random walk (Gut, 2009), which is essential for the applicability of the random sum LLN and CLT of Anscombe (1952). However, this rationale becomes untenable when the observations are contaminated by measurement errors such as market microstructure noise. In this section, we propose an empirically plausible approach to mitigate the noise. With a two-step noise reduction method, we transform the noise-contaminated observations into a sequence of pseudo-observations, which behaves locally like a Gaussian random walk in the limit. Since each

sampled return is only determined by finitely many tick-level returns within a local horizon, our test statistic that relies solely on the sample moments of normalized PDS returns remains valid.

To this end, we assume an additive noise term with a weak dependence structure, before which we recall the definition of α-mixing (Fan and Yao, 2003): The α-mixing coefficient of a stationary sequence $(X_i)_{i\in\mathbb{Z}}$ of variables indexed by $i \in \mathbb{Z}$ is defined as

$$\alpha(h) = \sup\{|\mathbb{P}(A \cap B) - \mathbb{P}(A)\mathbb{P}(B)| : A \in \mathcal{F}_i,\ B \in \mathcal{F}^{i+h}\}, \tag{24}$$

where the pre- and post-σ-fields are defined as $\mathcal{F}_j = \sigma(\{X_i : i \leq j\})$ and $\mathcal{F}^j = \sigma(\{X_i : i \geq j\})$. The process (X_i) is said to be α-mixing if $\alpha(h) \to 0$ as $h \to \infty$.

Assumption 3. Let $\varepsilon = (\varepsilon_i)_{0\leq i\leq N}$ be a stationary sequence with $\mathbb{E}[\varepsilon_i] = 0$ and $\mathbb{E}[|\varepsilon_i|^{2+\delta}] < \infty$ for some $\delta > 0$, where ε_i are identically distributed with variance σ_ε^2 and autocovariance function $\Gamma_h = \mathbb{E}[\varepsilon_i\varepsilon_{i+h}]$. The process ε is α-mixing with $\sum_{h=1}^{\infty} \alpha(h)^{\delta/2(2+\delta)} < \infty$, and exogenous to X. The sequence $Y = (Y_i)_{0\leq i\leq N}$ collects all observations contaminated by noise $Y_i = X_i + \varepsilon_i$, with the log-returns $r_i = Y_i - Y_{i-1}$ for all $1 \leq i \leq N$.

Remark 9. The autocovariance function Γ_h satisfies $\Gamma_0 = \sigma_\varepsilon^2$ and $\Gamma_{-h} = \Gamma_h$. For Γ_h, the standard absolute summability condition, i.e., $\sum_{h\in\mathbb{Z}} |\Gamma_h| < \infty$, is well-known to be sufficient for ergodicity and necessary for α-mixing under stationarity (Ibragimov and Linnik, 1971). Furthermore, the assumed conditions on the $(2+\delta)$-th moment and the α-mixing coefficient $\alpha(h)$ are sufficient for a CLT for the centered, stationary and α-mixing ε (Ibragimov, 1962; Theorem 8.3.7, Durrett, 2019).

Remark 10. The additive noise term ε_i summarizes a diverse array of market frictions. An i.i.d. additive noise with non-zero variance, firstly introduced by Zhou (1996), is commonly assumed in earlier literature of high-frequency volatility estimation, see, e.g., Aït-Sahalia et al. (2005) and Zhang et al. (2005). However, some previous studies including Hansen and Lunde (2006), Ubukata and Oya (2009), and Aït-Sahalia et al. (2011) find empirical evidence of self-dependent noise in financial markets. Recent work by Jacod et al. (2017) summarizes the common statistical properties of market microstructure noise and offers estimators for its autocovariances and autocorrelations, which further confirms this point. Assumption 3 allows for a weak dependence structure of the noise. This standard Itô semimartingale plus locally dependent noise framework has been employed by a number of recent studies, see, e.g., Jacod et al. (2017, 2019), Varneskov (2017), Christensen et al. (2022), and Li and Linton (2022).

However, it is worth noting that Assumption 3 is in fact more stringent than needed, given that Proposition 1 only necessitates the convergence of the pre-averaged returns defined in Eq. (25) to an α-mixing and stationary Gaussian process. This convergence result requires an appropriate limit theorem to hold for a weighted-average of the tick-level returns $r_i = \Delta_i^N Y = \Delta_i^N X + \Delta_i^N \varepsilon$, which is satisfied when the assumed α-mixing and stationary ε is exogenous to X. However, the same result holds when (r_i) itself satisfies such conditions for an appropriate limit theorem, which permits certain dependence structure between X and ε. For brevity, we will stick with the exogenous noise

assumption in the analysis henceforward, and examine its potential impact with a more general specification of ε via extensive simulations in Section 4.

With the additive noise under Assumption 3, the noisy observations clearly do not resemble a Gaussian random walk in the limit. There are two main problems:

(i) The noise term dominates the variance of tick-level returns (r_i) and does not shrink as $n \to \infty$;
(ii) The tick-level returns are no longer independent due to the self-dependence of ε.

We now introduce a two-step noise reduction method which facilitates the construction of a sequence of pseudo-observations with desirable properties:

Step 1: Pre-averaging. We implement the pre-averaging approach of Jacod et al. (2009): We choose a sequence of positive integers k_n satisfying $k_n\sqrt{\Delta_n} = \theta$ for some $\theta > 0$. We calculate log-returns on $(Y_i)_{0\le i\le N}$ that are pre-averaged in a local neighborhood of k_n observations:

$$r_i^* = \frac{1}{k_n}\sum_{j=k_n/2+1}^{k_n} Y_{i+j} - \frac{1}{k_n}\sum_{j=1}^{k_n/2} Y_{i+j} = \sum_{j=1}^{k_n-1} g\Big(\frac{j}{k_n}\Big) r_{i+j}, \tag{25}$$

where $g(s) = s \wedge (1-s)$, for all $i \in \{1,\dots,N'\}$ with $N' = N - 2k_n/2 + 2$.

Step 2: Random Sign Flip & Permutation. We compute the "wild-bootstrapped" returns based on the pre-averaged returns $(r_i^*)_{1\le i\le N'}$ obtained from Step 1:

$$\tilde{r}_i = r^*_{\pi(i)}\delta_{\pi(i)}, \tag{26}$$

where $(\delta_i)_{1\le i\le N'}$ is a sequence of i.i.d. Rademacher random variables,[6] and $\pi : \{1,\dots,N'\} \mapsto \{1,\dots,N'\}$ is a uniform random permutation of the index set $\{1,\dots,N'\}$.

Under the null, we show that the sequence of "wild-bootstrapped" returns $(\tilde{r}_i)_{1\le i\le N'}$ behave locally like a sequence of i.i.d. Gaussian random variables:

Proposition 1. Let ε, Y follow Assumption 3. Under the null hypothesis and as $n \to \infty$, the sequence $(\tilde{r}_i)_{1\le i\le N'}$ converges in distribution to a sequence of locally independent[7] and identically distributed Gaussian random variables with variances of order $\sqrt{\Delta_n}$.

Remark 11. We first discuss why this two-step method can mitigate the impact of noise under the null hypothesis. In Step 1, the standard choice of pre-averaging window balances the orders of X increments and ε, such that the pre-averaged returns $(r_i^*)_{1\le i\le N'}$ converges to a centered, stationary and self-dependent Gaussian process as $n \to \infty$. The dependence structure of (r_i^*) arises from both the assumed self-dependent ε and overlapping pre-averaging windows. Therefore, we proceed to

[6] A random variable $\delta \in \{-1, 1\}$ has a Rademacher distribution if $\mathbb{P}(\delta = -1) = \mathbb{P}(\delta = 1) = 1/2$.
[7] A formal definition of local independence is given in Eq. (A.62)

Step 2 to remove the local dependence, which is inspired by the wild bootstrap introduced by Wu (1986). The random sign flip eliminates serial correlations in (r_i^*). The uniform random permutation assigns equal probability to each of the $N'!$ possible permutations, which ensures that any two variables in $(\tilde{r}_i)_{1\leq i\leq N'}$ are independent when their indices are not sufficiently far apart from each other in $\{1,\ldots,N'\}$ under infill asymptotics.

Proposition 1 inspires the construction of our test in the presence of noise as follows: We generate a sequence of pseudo-observations $(\tilde{Y}_i)_{0\leq i\leq N'}$ as partial sums of $(\tilde{r}_i)$, where $\tilde{Y}_0 = Y_0$ and $\tilde{Y}_i = \sum_{j=1}^{i} \tilde{r}_j$. Next, we choose a sequence of barrier widths $c = m\Delta_n^{1/4}$ and obtain the sampled observations $(\tilde{Y}_i^{(c)})$. Finally, we follow Section 3.1 to construct the standardized test statistic $\tilde{T}_{c,\epsilon}$ from $(\tilde{Y}_i^{(c)})$ in place of $(X_i^{(c)})$. Formal establishment of its asymptotic properties requires further assumptions about the noise, and is left for future research. We discuss some plausible properties of $\tilde{T}_{c,\epsilon}$ in the two Remarks below, which are verified through comprehensive simulations with a realistically calibrated noise specification in the next section.

Remark 12. The choice of $c = m\Delta_n^{1/4}$ ensures that the normalized increments $\tilde{r}_i/c$ are invariant to Δ_n, which is analogous to the case without noise. Assuming that $(\tilde{r}_i)_{1\leq i\leq N'}$ is a sequence of i.i.d. centered Gaussian random variables, $(\tilde{Y}_i)_{0\leq i\leq N'}$ forms a genuine Gaussian random walk, and thus the same CLT in Theorem 2 would hold for $\tilde{T}_{c,\epsilon}$ under the null. Our simulation results reveal that this CLT still holds for $\tilde{T}_{c,\epsilon}$ constructed from $(\tilde{Y}_i)$. This is because each sampled return is only determined by finitely many increments of $(\tilde{Y}_i)$ within a local horizon, which are indeed asymptotically i.i.d.. Importantly, the convergence rate of $\tilde{T}_{c,\epsilon}$ remains $\sqrt{N}$, which apparently contradicts to the optimal $N^{1/4}$ rate of noise-robust IV estimators (Gloter and Jacod, 2001; Xiu, 2010; Reiß, 2011) that also appear in some noise-robust jump tests (Aït-Sahalia et al., 2012). This discrepancy arises because our test statistic does not rely on a noise-robust IV estimator, but rather on a consistent estimator of the scale-invariant barrier width m, which is identified through the variance of $\tilde{r}_i$. As $\tilde{r}_i$ has the same order as the pre-averaged noise, a consistent estimator of m has the same $\sqrt{N}$ rate as that of a noise variance estimator. Consequently, the estimator of m cannot be translated into a consistent IV estimator in the spirit of Remark 8 when noise exists. Nevertheless, this finding also reveals that a noise-robust IV estimator is not a pre-requisite for noise-robust jump tests.

Remark 13. When X is discontinuous on $(0,1)$, we conjecture that our test remains consistent under the alternative hypothesis of local-to-infinite-activity jumps, although it may require a more stringent assumption on u_n in Eq. (7). For example, the order of the pre-averaged returns $\tilde{r}_i$ becomes $\Delta_n^{1/4}$, such that u_n needs to satisfy $u_n\Delta_n^{-1/4} \to \infty$ and $u_n\Delta_n^{\beta-1/2} \to 0$ for any $\beta \in (1/4, 1/2]$ as $n \to \infty$ to exclude all jumps that shrink either faster than or equal to the pre-averaged returns from the alternative hypothesis.

4 Monte Carlo Simulations

4.1 Simulation Design

We simulate an empirically realistic discretized diffusion model for asset prices, which incorporates both time varying tick-variances and transaction activities. Firstly, we simulate a Heston model for the efficient price process X and obtain its tick-level observations, to which we add jumps with different sizes:

$$\begin{aligned} dX_t &= \Big(\mu - \frac{\sigma_t^2}{2}\Big)dt + \sigma_t dW_t + dX_t'', \quad t \in [0,1] \\ d\sigma_t^2 &= \alpha(\theta - \sigma_t^2)dt + \eta\sigma_t dB_t, \end{aligned} \tag{27}$$

where $W = (W_t)$ and $B = (B_t)$ are standard Brownian motions with $\mathrm{Corr}(W_t, B_t) = \rho$, and X'' is a compound Poisson process, i.e.,

$$X_t'' = \sum_{i=1}^{N_t} J_i, \tag{28}$$

where $N = (N_t)$ is a Poisson process with rate λ, and jump sizes J_i follow a double exponential distribution (Laplace distribution) with the location parameter 0 and the scale parameter b. To generate all tick-level observations, we discretize X equidistantly on $t = i/n$ for $n = 23,400$. Then we modify the observation times $0 \leq t_{n,1} < t_{n,2} < \cdots \leq 1$ following an inhomogeneous Poisson process with the rate

$$\alpha(t) = 1 - \frac{1}{2}\cos 2\pi t, \tag{29}$$

where $t \in [0,1]$. The inverted U-shaped rate function $\alpha(t)$ is employed to mimic the empirical feature of more transactions that occur in the early morning and late afternoon than in the middle of the trading day (Jacod et al., 2017). We draw 10,000 simulated price paths for each experiment.

For the additive noise,[8] we denote

$$\varepsilon_i = 2\sqrt{\frac{\sigma_{t_{n,i}}^2}{n}}\left(\omega_i^A + \omega_i^B\sqrt{\frac{\nu-2}{\nu}}\right), \tag{30}$$

where ω_i^A are autocorrelated Gaussian random variables defined as

$$\omega_i^A = \phi_i + \sum_{j=1}^{\Lambda}\beta_j\phi_{i-j}, \quad \text{with } \phi_i \sim \text{i.i.d.}\,\mathcal{N}(0,1), \text{ and } \beta_j = \frac{d(1+d)\cdots(j-1+d)}{j!}, \tag{31}$$

for $d \in (-0.5, 0.5)$ and a large cutoff value Λ, which form a moving-average series that approximates a fractionally differenced process (Jacod et al., 2019), and ω_i^B are i.i.d. draws from a Student's t

[8] The simulation design of additive noise mainly follows Aït-Sahalia et al. (2012). In addition, we consider its serial correlation using the method of Jacod et al. (2019).

distribution with the degree of freedom ν.

The instantaneous standard deviation of the Gaussian-t mixture noise is about four times as much as that of diffusive increments, i.e., $\sqrt{\sigma^2_{t_{n,i}}/n}$, so that the diffusive increments are clearly dominated by the additive noise.[9] This specification of ε_i captures some important features of market microstructure noise in financial markets, e.g., temporal heteroscedasticity, slowly-decaying serial correlation, intraday seasonality, and dependence on the latent prices. The t-distributed noise ω_i^B is introduced to capture the large bouncebacks commonly observed in high-frequency transaction data (Aït-Sahalia et al., 2012). Besides the additive noise, we also consider the rounding errors on the price level, i.e., let the observed prices $e^{Y_i} = e^{X_i+\varepsilon_i}$ be further rounded to cents. The observed logarithmic prices are given as

$$Y_i = \log\left(\left[\frac{e^{X_i+\varepsilon_i}}{0.01}\right] \times 0.01\right), \tag{32}$$

where the function $[x]$ rounds a number x to the nearest integer.[10]

The annualized parameters for the Heston model are fixed at $(\mu, \alpha, \theta, \eta, \rho) = (0.05, 5, 0.16, 0.5, -0.5)$, where the volatility parameters satisfy the Feller's condition $2\alpha\theta \geq \eta^2$ which ensures the positivity of σ. The parameter choices follow both Aït-Sahalia and Jacod (2009) and Aït-Sahalia et al. (2012), which are calibrated according to the empirical estimates in Aït-Sahalia and Kimmel (2007). For the jump components, we let $\lambda = 1$, and $b = 0.2\sqrt{\theta}$ and $0.4\sqrt{\theta}$ corresponding to moderate and relatively large jump sizes. The moderate (resp. large) jumps contribute about 7% (resp. 25%) of the daily QV on average when noise is absent. For the additive noise term, we let $(d, \Lambda, \nu) = (0.3, 100, 2.5)$ following Aït-Sahalia et al. (2012) and Jacod et al. (2019).

Fig. 3 depicts the intraday variation of some market activity variables of a simulated path in the absence of noise, which include the return, number of trades, and annualized RV in each one-minute interval. Both transaction intensity and return variation exhibit a U-shaped pattern over the trading hours, which is in line with some prior empirical findings (Harris, 1986; Wood et al., 1985; Andersen and Bollerslev, 1997; Andersen et al., 2018, 2019, 2023). Fig. 4 compares the simulated tick-level latent prices and the rounded, noise-contaminated price observations over an intraday episode.

4.2 Test Performance in the Absence of Market Microstructure Noise

Table 1 reports the finite-sample size and size-adjusted power (at 5% nominal level) of the standardized test statistic $T_{c,\epsilon}$ when noise is absent. Tick-level observations are sampled with different PDS barrier widths $c = K\sigma(r_i)$, i.e., K times the standard deviation of tick-by-tick returns, where K ranges from 3 to 10. Different censoring thresholds with $\epsilon \in \{0.05, 0.07, 0.1\}$ are also considered. In Table 1, the rejection rates under the null (Panel A) are all closely align with the nominal level. For the finite-sample power under the alternative (Panels B and C), we find that the rejection rates are

[9] In the simulations, we follow Aït-Sahalia et al. (2012) to truncate the t-distributed ω_i^B at $\pm 50\sqrt{\nu/(\nu-2)}$ to avoid large returns in the absence of jumps, which could lead to very misleading results. Hence, the instantaneous standard deviation of the t-distributed noise $2\omega_i^B\sqrt{\sigma^2_{t_{n,i}}/n}\sqrt{(\nu-2)/\nu}$ is slightly lower than $2\sqrt{\sigma^2_{t_{n,i}}/n}$.

[10] We also consider alternative specifications for the additive heteroscedastic noise, see the results in Appendix B.2.

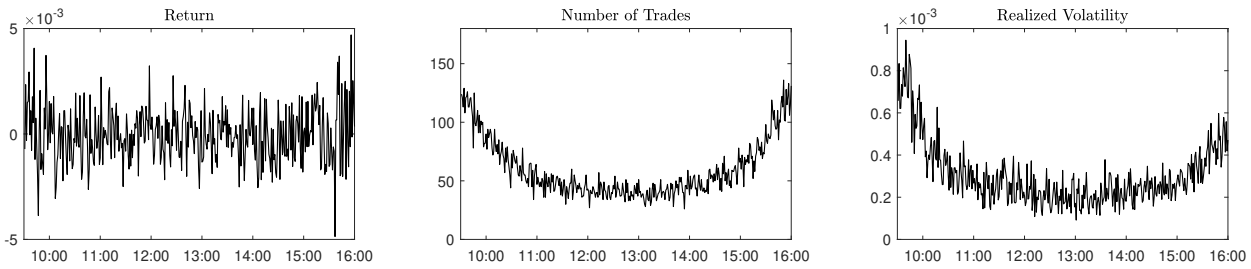

Figure 3: Some market activity variables of simulated prices. The tick-level observations are simulated with the Heston model in Eq. (27), and we assign randomized observation times with an inverted U-shape rate function in Eq. (29) to all observations. The returns, numbers of transactions, and annualized RVs are computed at a granularity of one minute.

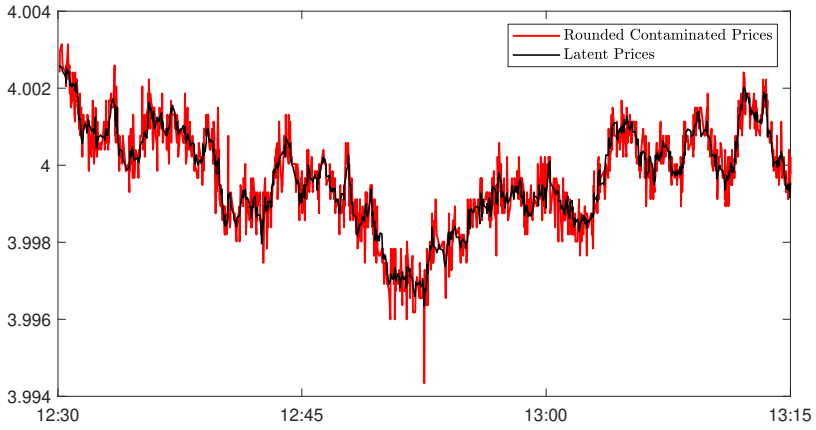

Figure 4: Comparison of the simulated latent prices and the noise-contaminated prices with rounding errors.

fairly robust across different sampling frequencies. Fig. 5 compares the finite-sample distributions of our test statistic with the limiting standard normal distribution. Under the null, the finite-sample distribution (solid line) closely resembles the standard normal (shaded area), while the distribution deviates significantly from $\mathcal{N}(0,1)$ when there exist jumps of either moderate or large sizes.

Table 1: Finite-sample size and power (%)

Nominal size: 5%	Panel A No Jump				Panel B Moderate Price Jumps				Panel C Large Price Jumps			
		ϵ				ϵ				ϵ		
$c/\sigma(r_i)$	$N^{(c)}$	0.05	0.07	0.10	$N^{(c)}$	0.05	0.07	0.10	$N^{(c)}$	0.05	0.07	0.10
3	1786	5.26	5.31	5.48	1697	58.21	61.68	65.22	1564	76.29	78.47	80.37
4	1100	5.51	5.58	5.89	1043	61.24	64.54	67.46	959	77.95	80.18	81.99
5	744	5.39	5.56	5.77	705	63.01	66.29	69.55	647	79.10	81.00	82.83
6	536	4.99	5.20	5.61	508	63.77	67.13	70.30	466	80.16	82.01	83.92
7	405	5.28	5.56	5.71	383	65.19	68.47	71.07	351	80.59	82.23	84.01
8	316	5.20	5.61	5.93	299	65.86	68.90	72.07	274	80.76	82.51	84.36
9	254	5.28	5.46	6.01	240	66.33	68.88	71.47	220	81.36	82.78	84.42
10	208	5.07	5.29	5.49	197	66.66	69.33	72.16	181	81.20	83.18	84.85

This table reports the finite-sample size and size-adjusted power (%) of 10,000 simulations of the test statistic $T_{c,\epsilon}$ at 5% nominal level in the absence of market microstructure noise. Tick-level observations are sampled with different PDS barrier widths $c = K\sigma(r_i)$, i.e., K times the standard deviation of tick-by-tick returns, where K ranges from 3 to 10. Different censoring thresholds with $\epsilon \in \{0.05, 0.07, 0.1\}$ are considered. $N^{(c)}$ stands for the average sampling frequencies.

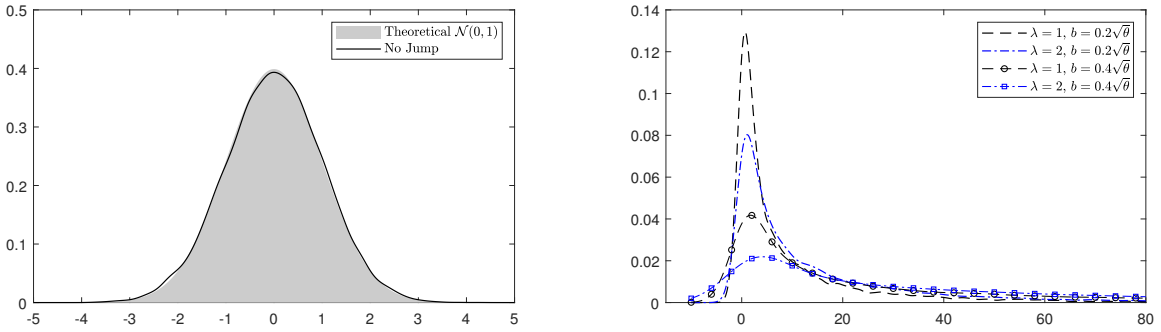

Figure 5: Finite-sample distributions of the standardized test statistic $T_{c,\epsilon}$. We plot the finite-sample distribution under the null (solid line) and compare it with the simulated standard normal (shaded area). Jumps are simulated with a compounded Poisson process with the intensity λ, and their sizes follow a double exponential distribution with the location parameter 0 and the scale parameter b. We consider different parameter choices: (i) $\lambda = 1$, $b = 0.2\sqrt{\theta}$ (dash), (ii) $\lambda = 2$, $b = 0.2\sqrt{\theta}$ (dash-dot), (iii) $\lambda = 1$, $b = 0.4\sqrt{\theta}$ (dash-circle), and (iv) $\lambda = 2$, $b = 0.4\sqrt{\theta}$ (dash-square). In all cases, the PDS barrier width $c = 5\sigma(r_i)$, and the censoring parameter $\epsilon = 0.05$.

4.3 Test Performance in the Presence of Market Microstructure Noise

Panel A in Table 2 summarizes the finite-sample size (at 5% nominal level) of the standardized test statistic $T_{c,\epsilon}$ constructed from the rounded noise-contaminated observations. We employ the two-step noise reduction method in Section 3.2 to construct the sequence of pseudo-observations with three different pre-averaging windows, i.e., $k_n = \lceil \theta\sqrt{N} \rceil$ with $\theta \in \{0.3, 0.4, 0.5\}$. The choices of θ follow the rule of thumb in Hautsch and Podolskij (2013). Similar to the results in the absence of noise, the rejection rates under the null are close to the nominal level across almost all choices of bandwidth c and censoring parameter ϵ. Panels B and C in Table 2 report the size-adjusted power under the alternative with moderate and large jumps, respectively. Compared with the simulation results in Table 1, the finite-sample power experiences a marginal reduction but remains above 40% for most of the parameter choices. Fig. 6 compares the finite-sample distributions of $T_{c,\epsilon}$ with $\mathcal{N}(0,1)$. It is observed that $T_{c,\epsilon}$ is almost a standard normal under the null, but it has a notably larger magnitude than $\mathcal{N}(0,1)$ under the alternative. Compared this with Fig. 5, we observe that the right tails of the test statistic become smaller with the same jump specifications. This explains the slightly reduced power of our test in the presence of market microstructure noise.

We then compare the empirical rejection rates of our test with those of 9 classical high-frequency jump tests constructed from equidistantly calendar-time-sampled observations (Table 3). These tests include BNS (Barndorff-Nielsen and Shephard, 2006), ABD (Andersen et al., 2007b), JO (Jiang and Oomen, 2008), LM (Lee and Mykland, 2008), ASJ (Aït-Sahalia and Jacod, 2009), CPR (Corsi et al., 2010), PZ (Podolskij and Ziggel, 2010), MinRV and MedRV (Andersen et al., 2012). The parameter choices for all these tests are determined in accordance with the recommendations from their original literature.[11] Our analysis, in line with the Monte Carlo results of Dumitru and Urga (2012) and Maneesoonthorn et al. (2020), demonstrates that nearly all the tests constructed

[11] Some parameter choices are reported in Appendix B.1.

Table 2: Finite-sample size and power (%)

Nominal size: 5%		$\theta = 0.3$				$\theta = 0.4$				$\theta = 0.5$			
			ϵ				ϵ				ϵ		
	$c/\sigma(\tilde{r}_i)$	$N^{(c)}$	0.05	0.07	0.10	$N^{(c)}$	0.05	0.07	0.10	$N^{(c)}$	0.05	0.07	0.10
Panel A No Jump	3	1784	4.90	5.15	5.20	1784	4.80	5.35	5.71	1783	5.06	5.07	5.70
	4	1099	4.84	4.95	5.42	1098	5.29	5.10	5.51	1098	5.14	5.08	5.79
	5	743	4.94	5.01	5.20	743	5.19	5.02	5.57	742	4.81	5.02	5.70
	6	536	4.74	4.89	5.57	536	4.78	5.11	5.58	535	4.96	5.11	5.47
	7	404	4.99	5.11	5.29	404	4.86	5.05	5.76	404	4.86	5.17	5.46
	8	316	5.15	5.37	5.54	316	4.82	5.08	5.43	315	4.81	5.30	5.82
	9	253	5.04	5.41	5.13	254	4.84	5.10	5.63	253	4.96	5.28	5.73
	10	208	5.18	5.10	5.60	208	4.84	5.34	5.54	208	5.04	5.08	5.66
Panel B Moderate Jump	3	1716	46.00	49.28	51.77	1717	44.98	46.84	49.27	1718	43.08	45.18	47.52
	4	1058	45.89	48.56	50.92	1059	43.31	46.76	48.56	1061	41.35	44.77	46.22
	5	717	44.95	47.45	50.42	719	42.99	45.50	47.53	720	40.81	43.12	44.93
	6	519	44.60	46.65	48.86	519	42.82	43.97	47.01	520	40.25	42.06	45.01
	7	392	43.79	45.31	48.98	393	41.00	43.15	46.29	394	40.08	41.95	45.04
	8	307	42.45	45.21	48.64	308	40.97	42.47	46.81	308	39.98	41.03	43.83
	9	247	41.38	43.95	48.57	248	40.54	42.58	45.62	248	38.45	41.21	43.67
	10	203	41.08	44.57	47.51	204	40.04	41.30	45.45	204	38.12	40.03	43.86
Panel C Large Jump	3	1594	68.85	70.38	72.44	1596	68.06	69.14	70.54	1599	66.37	68.54	69.68
	4	983	68.79	70.51	72.17	986	66.37	68.97	70.42	990	65.60	67.26	68.97
	5	668	67.26	69.92	71.80	671	66.37	68.22	69.52	673	65.11	66.50	68.19
	6	484	67.69	69.41	70.48	486	65.92	67.13	69.67	489	64.38	66.05	68.07
	7	367	66.78	68.71	70.81	369	65.14	66.46	68.54	371	63.68	65.35	67.61
	8	288	65.84	68.11	70.24	290	64.22	66.40	68.42	292	62.93	64.89	66.90
	9	233	65.83	67.44	70.32	234	64.08	66.29	68.38	236	62.29	64.68	66.67
	10	192	65.00	66.96	69.70	193	63.44	65.54	68.23	194	61.91	64.12	66.69

This table reports the finite-sample size and size-adjusted power (%) of 10,000 simulations of the test statistic $T_{c,\epsilon}$ at 5% nominal level. All simulated prices are contaminated by the additive Gaussian-t mixture noise and rounding errors. We utilize the two-step noise reduction method in Section 3.2 to construct the sequence of pseudo-observations with three different pre-averaging windows, i.e., $k_n = \lceil \theta\sqrt{N} \rceil$ with $\theta \in \{0.3, 0.4, 0.5\}$. The observations are sampled with different PDS barrier widths $c = K\sigma(\tilde{r}_i)$, where K ranges from 3 to 10. Different censoring thresholds with $\epsilon \in \{0.05, 0.07, 0.1\}$ are considered. $N^{(c)}$ stands for the average sampling frequencies.

from equidistantly sampled observations suffer from size distortion and their results become highly unstable under the assumed additive Gaussian-t mixture noise and rounding errors. This noise significantly distorts their finite-sample null distributions, particularly at higher sampling frequencies. It might be interesting to see that the size of the JO test is close to the nominal level. However, a closer examination reveals that this is caused by two cancelling distortions due to the mixture of Gaussian and t-distributed noise specification, see Appendix B.2 for details. While sparse sampling can alleviate size distortion, it also substantially weakens the power of these tests.

For more appropriate benchmarks when the noise is present, we also consider some noise-robust versions of classical tests (Table 4) constructed from ultra-high-frequency data: the noise-adjusted PZ (Podolskij and Ziggel, 2010), LM12 (Lee and Mykland, 2012), and ASJL (Aït-Sahalia et al., 2012). Similar to our test, all these noise-robust tests rely on the pre-averaging approach of Jacod

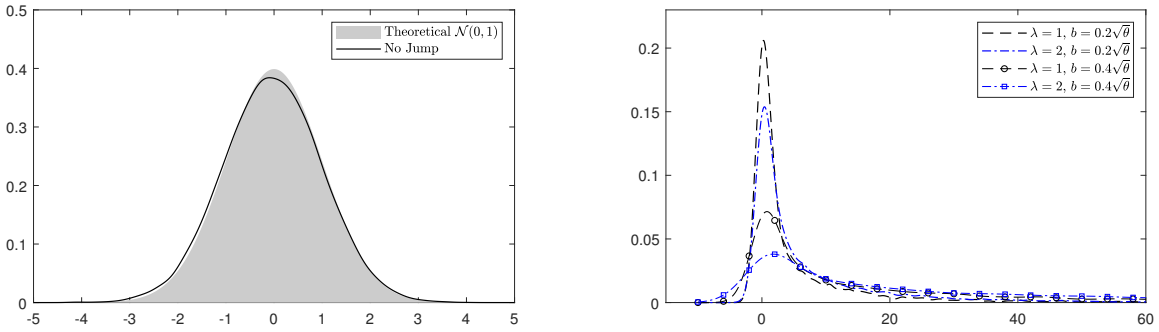

Figure 6: Finite-sample distributions of the standardized test statistic $T_{c,\epsilon}$ in the presence of noise. We plot the finite-sample distribution under the null (solid line) and compare it with the simulated standard normal (shaded area). Jumps are simulated with a compounded Poisson process with the intensity λ, and their sizes follow a double exponential distribution with the location parameter 0 and the scale parameter b. We consider different parameter choices: (i) $\lambda = 1$, $b = 0.2\sqrt{\theta}$ (dash), (ii) $\lambda = 2$, $b = 0.2\sqrt{\theta}$ (dash-dot), (iii) $\lambda = 1$, $b = 0.4\sqrt{\theta}$ (dash-circle), and (iv) $\lambda = 2$, $b = 0.4\sqrt{\theta}$ (dash-square). In all cases, we select the pre-averaging window $k_n = \lceil \theta\sqrt{N} \rceil = 46$ with $\theta = 0.3$, the PDS barrier width $c = 5\sigma(\tilde{r}_i)$, and the censoring parameter $\epsilon = 0.05$.

Table 3: Finite-sample size and power (%) of other tests

Nominal size: 5%											
	Int. (sec)	N_{spl}	BNS	ABD	JO	LM	ASJ	CPR	PZ	MinRV	MedRV
Panel A No Jump	5	4680	0.33	98.53	6.19	98.40	99.98	33.39	89.61	0.00	0.00
	15	1560	0.42	71.96	5.23	71.12	99.42	18.20	52.91	0.00	0.12
	30	780	3.30	45.63	5.25	46.82	76.71	13.02	30.25	0.99	2.53
	60	390	5.16	28.49	5.75	30.82	29.50	8.47	19.57	3.35	5.30
	120	195	6.46	21.02	8.08	17.73	10.60	7.86	16.76	4.78	6.91
	180	130	6.90	18.61	8.95	15.10	7.52	8.05	15.96	5.29	8.16
	300	78	7.65	15.93	10.87	12.12	4.84	8.97	15.58	5.34	8.98
Panel B Moderate Jump	5	4680	30.08	99.58	31.95	15.80	97.25	10.93	12.40	16.91	26.45
	15	1560	36.42	88.73	36.33	24.78	94.76	21.13	20.59	32.89	36.17
	30	780	33.20	74.27	33.89	32.00	77.29	28.64	28.39	28.95	33.25
	60	390	28.25	61.69	28.25	36.63	45.44	29.58	37.36	24.96	28.61
	120	195	21.64	48.76	20.90	32.73	24.43	24.18	30.47	20.07	23.51
	180	130	17.40	42.22	17.16	28.97	16.57	19.34	25.51	16.34	19.42
	300	78	13.83	33.48	11.33	20.56	11.44	15.93	19.09	13.32	14.74
Panel C Large Jump	5	4680	56.35	99.81	59.11	43.00	95.12	32.58	36.63	42.72	53.55
	15	1560	60.94	93.98	61.18	52.39	95.31	47.32	47.58	58.68	60.84
	30	780	59.06	86.29	59.05	58.46	83.73	54.54	55.57	54.79	58.43
	60	390	54.36	78.40	54.57	62.78	59.83	56.25	62.88	50.60	54.90
	120	195	46.78	70.17	46.16	58.81	36.76	50.12	56.74	44.11	49.20
	180	130	41.21	64.64	40.86	54.93	26.94	44.83	51.91	39.32	44.13
	300	78	34.07	55.92	33.19	45.73	16.14	38.76	43.76	33.66	37.49

This table reports the finite-sample size and size-adjusted power (%) of 10,000 simulations of 9 classical tests at 5% nominal level: BNS (Barndorff-Nielsen and Shephard, 2006), ABD (Andersen et al., 2007b), JO (Jiang and Oomen, 2008), LM (Lee and Mykland, 2008), ASJ (Aït-Sahalia and Jacod, 2009), CPR (Corsi et al., 2010), PZ (Podolskij and Ziggel, 2010), MinRV and MedRV (Andersen et al., 2012). All these tests are constructed on observations equidistantly sampled with various intervals in calendar time: 5, 15, 30, 60, 120, 180 and 300 seconds, and "N_{spl}" stands for the sampling frequencies.

et al. (2009) to "pre-filter" the noise-contaminated observations.[12] The "optimal" tuning parameters

[12] With a simplified i.i.d. noise specification, Andersen et al. (2007b) introduce an "event time" correction of ABD, and Jiang and Oomen (2008) propose an analytically modified form of JO. However, both of them cannot achieve comparable performance under the simulated Gaussian-t mixture noise.

for those tests are selected by minimizing the absolute distance between the nominal size and the empirical size with the simulated tick-level noise-contaminated observations.[13]

Table 4: Finite-sample size and power (%) of other noise-robust tests

Nominal size: 5%					
	Int. (sec)	N_{spl}	PZ*	LM12	ASJL
No Jump	tick	23400	5.29	5.03	5.12
	5	4680	4.96	8.83	8.79
Moderate Jump	tick	23400	38.57	22.70	38.22
	5	4680	30.38	18.79	17.66
Large Jump	tick	23400	64.78	40.76	63.50
	5	7680	56.49	31.38	41.96

This table reports the finite-sample size and size-adjusted power (%) of 10,000 simulations of 3 noise-robust tests at 5% nominal level: noise-adjusted PZ (Podolskij and Ziggel, 2010), LM12 (Lee and Mykland, 2012), and ASJL (Aït-Sahalia et al., 2012). All these tests are constructed on tick-level and 5-second-sampled observations. The tuning parameters for those tests are selected by minimizing the absolute distance between the nominal size and the empirical size with the simulated tick-level noise-contaminated observations.

As illustrated in Table 2, our PDS-based test demonstrates robustness across various parameter choices: (i) barrier width c, (ii) censoring parameter ϵ, and (iii) pre-averaging window $k_n = \lceil \theta\sqrt{N} \rceil$, even when we consider such a complicated and realistic noise specification. Furthermore, our test remains competitive and, often superior, to those noise-robust tests with optimal parameter choices. While we refrain from providing optimal parameter choices, we offer recommended ranges for practitioners:

(i) Choose c as a multiple of the standard deviation of $\tilde{r}_i$, i.e., $c = K\sigma(\tilde{r}_i)$, with $3 \leq K \leq 10$.
(ii) Choose ϵ in $[0.03, 0.15]$.
(iii) Choose the pre-averaging window $k_n = \lceil \theta\sqrt{N} \rceil$ with $\theta \in [0.2, 0.8]$.

Through extensive simulation studies with different specifications of market frictions, we believe that the recommended parameter choices work reasonably well in finite samples when the number of intraday tick-level observations is no less than 10,000. Additional simulation results can be found in Appendix B.2.

5 Empirical Analysis

In this section, we employ our new jump test on the high-frequency transaction data of 10 stocks listed on the New York Stock Exchange (NYSE): American Express (AXP), Boeing (BA), Disney (DIS), IBM, Johnson & Johnson (JNJ), JP Morgan (JPM), Merck (MRK), McDonald's (MCD), Procter & Gamble (PG), and Walmart (WMT). Our Trade and Quote (TAQ) dataset includes all transactions from 9:30 am to 4:00 pm on each trading day in 2020. As is standard in empirical

[13] Note that the optimal tuning parameters are not empirically feasible in practice. Therefore, the results presented should be interpreted as theoretical upper bounds for these benchmark tests.

research involving high-frequency financial data, we apply filters, as outlined in Barndorff-Nielsen et al. (2009), to eliminate clear data errors, remove all transactions in the original record that are later corrected, cancelled or otherwise invalidated, and keep transactions on NYSE only. Table 5 reports descriptive statistics of trades on these selected NYSE stocks, which include the number of trades, observed transaction prices in dollar terms, and intraday log-returns in basis points. Our PDS-based test utilizes the same tuning parameters as those in Section 4: the PDS barrier width $c = K\sigma(\tilde{r}_i)$ with K ranging from 4 to 6, the censoring parameter $\epsilon = 0.05$, and three pre-averaging windows $k_n = \lceil \theta\sqrt{N} \rceil$ with $\theta \in \{0.3, 0.4, 0.5\}$.

Table 5: Descriptive statistics of daily trades on selected NYSE stocks

Stock		AXP	BA	DIS	IBM	JNJ
Number of trades	Min	3171	10556	9785	5047	6383
	Max	59273	245802	125550	49178	71733
	Mean	19351	55314	37962	17818	22966
	Std Dev	9205	38352	20390	8265	11561
Trasaction prices	Min	67.03	89.00	79.07	90.56	109.16
	Max	138.16	349.45	183.40	158.78	157.66
	Mean	100.88	181.46	121.78	123.16	143.33
	Std Dev	14.72	51.15	20.12	11.57	8.53
Intraday log-returns (1×10^{-4})	Min	−123.24	−163.29	−100.49	−143.49	−110.04
	Max	97.48	129.22	75.30	143.49	200.25
	Mean	0.00	0.00	0.00	0.00	0.00
	Std Dev	1.78	1.85	1.17	1.44	1.23
Stock		JPM	MRK	MCD	PG	WMT
Number of trades	Min	12593	5787	3968	7516	9845
	Max	156987	71570	55024	76337	90546
	Mean	44738	22833	16096	23224	26148
	Std Dev	25335	11058	7838	10422	13032
Trasaction prices	Min	76.92	65.26	124.23	94.31	102.00
	Max	141.10	92.14	231.91	146.92	153.60
	Mean	103.17	79.86	195.17	125.19	128.55
	Std Dev	14.28	4.55	21.74	11.63	12.04
Intraday log-returns (1×10^{-4})	Min	−103.80	−177.00	−154.39	−132.25	−305.08
	Max	103.80	117.50	142.80	207.58	190.19
	Mean	0.00	0.00	0.00	0.00	0.00
	Std Dev	1.06	1.26	1.74	1.33	1.13

This table contains summary statistics for the number of trades, observed transaction prices in dollars, and intraday log-returns in basis points for 10 selected NYSE stocks in 2020. Data are collected from the TAQ database which includes all transactions from 9:30 am to 4:00 pm in each trading day. We apply filters, as outlined in Barndorff-Nielsen et al. (2009), to eliminate clear data errors, remove all transactions in the original record that are later corrected, cancelled or otherwise invalidated, and keep transactions on NYSE only.

Table 6 reports the proportions of trading days with rejections in 2020, as determined by our PDS-based test. For the selected stocks, the proportions of trading days with identified jumps are no more than 20%, with only AXP and MCD identified to exhibit over 15% of trading days containing jumps. There is little variation of the rejection rates across different stocks, and the results are relatively stable with different parameter choices. For each stock, there is a slight decrease in the percentage of identified jumps when we employ a larger barrier width c for PDS, i.e., sample less frequently. To visualize the testing results for the selected stocks in 2020, we aggregate all stock-day

outcomes, which yields a total of 2530 stock-day pairs. Fig. 7 illustrates the empirical distributions of the standardized test statistic (solid line) and compares it with the standard normal distribution $\mathcal{N}(0,1)$. Relative to the limiting distribution under the null hypothesis of no jump (shaded area), the empirical distribution of our test statistic deviates slightly towards the right side, but maintainss a bell shape centered around 0.5.

Table 6: Empirical rejection rates (%) for selected NYSE stocks

k_n	$c/\sigma(\tilde{r}_i)$	AXP	BA	DIS	IBM	JNJ	JPM	MRK	MCD	PG	WMT
	4	17.00	10.67	9.88	13.04	13.83	10.67	10.67	16.60	13.44	11.07
$\theta = 0.3$	5	15.81	10.67	9.49	12.25	11.86	10.67	10.28	16.21	11.86	10.67
	6	14.23	9.88	9.09	12.25	11.46	10.28	9.88	15.02	11.86	11.07
	4	16.21	9.88	10.28	13.44	12.65	10.67	9.88	15.81	12.65	12.25
$\theta = 0.4$	5	15.02	9.88	9.49	12.25	12.25	10.67	9.49	15.42	11.86	11.07
	6	14.23	9.49	9.49	11.46	11.07	9.88	9.49	14.23	11.46	10.28
	4	15.81	10.28	10.28	12.25	13.04	10.28	10.28	15.81	12.25	11.46
$\theta = 0.5$	5	14.23	9.09	9.88	12.25	11.46	9.49	9.09	15.02	11.86	10.67
	6	13.44	8.70	9.09	11.46	11.07	9.88	9.09	14.62	11.07	10.67

This table reports the proportions of days with jumps identified by the PDS-based test for 10 NYSE stocks in 2020. We use three pre-averaging windows $k_n = \lceil \theta\sqrt{N} \rceil$ with $\theta \in \{0.3, 0.4, 0.5\}$, different PDS barrier widths $c = K\sigma(\tilde{r}_i)$, i.e., the integer multiple of the standard deviation of pre-averaged returns, with K ranging from 4 to 6, and the censoring parameter $\epsilon = 0.05$. The total number of trading days is 253.

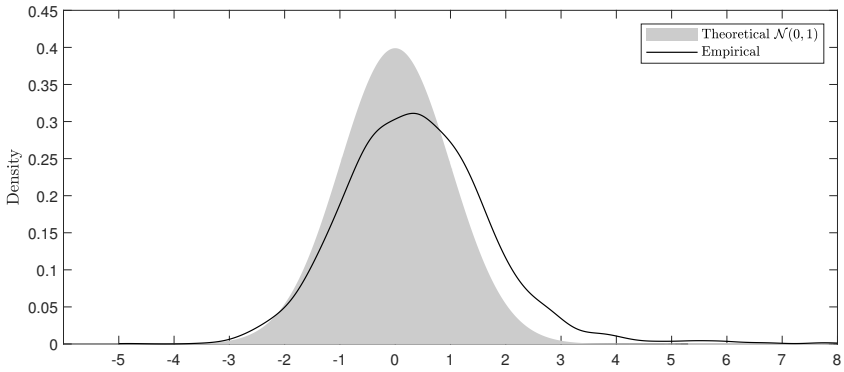

Figure 7: Testing results for selected NYSE stocks in 2020. We plot the empirical distribution of the standardized test statistic for all 2530 stock-day pairs and, for comparison, the simulated standard normal distribution (shaded area). We use the PDS barrier width $c = 4\sigma(\tilde{r}_i)$, the censoring parameter $\epsilon = 0.05$, and the pre-averaging window $k_n = \lceil \theta\sqrt{N} \rceil$ with $\theta = 0.3$, which corresponds to the first row in Table 6.

To eliminate spurious detections due to the multiple testing issue, Bajgrowicz et al. (2016) propose a formal treatment of the over-identification bias with double asymptotics when the jump tests are applied over a sample of many days. We apply their thresholding methods to our results: (i) the universal threshold $\sqrt{2\ln 253}$, and (ii) the threshold based on the false discovery rate (FDR).[14]

[14] For the vector of one-side test statistics $(S_1, S_2, \ldots, S_N)'$ which converge to i.i.d. standard normal random variables under the null, the universal threshold is $\sqrt{2\ln N}$ (Bajgrowicz et al., 2016). The data-adaptive FDR threshold is determined from the observed p-value distribution by the Benjamini–Hochberg procedure.

Table 7: Adjusted empirical rejection rates (%) for selected NYSE stocks

	k_n	$c/\sigma(\tilde{r}_i)$	AXP	BA	DIS	IBM	JNJ	JPM	MRK	MCD	PG	WMT
Panel A Universal threshold	$\theta = 0.3$	4	15.02	9.49	9.09	12.25	12.25	7.91	9.49	14.62	11.07	9.49
		5	13.83	9.88	8.70	11.07	10.28	8.30	9.09	14.62	9.88	8.70
		6	12.65	8.70	8.30	11.07	10.28	7.91	8.70	13.44	9.88	9.09
	$\theta = 0.4$	4	14.23	8.70	9.49	12.25	11.07	8.30	8.70	14.23	10.28	9.88
		5	13.44	8.70	8.70	11.46	11.07	8.30	8.30	13.83	9.88	9.09
		6	13.04	8.70	8.70	10.67	9.88	7.91	8.30	12.65	9.49	8.70
	$\theta = 0.5$	4	13.83	9.09	9.09	11.46	11.86	8.30	9.09	13.83	10.28	9.49
		5	12.65	8.30	9.09	11.07	10.28	7.51	7.91	13.44	9.88	8.70
		6	11.86	7.91	8.30	10.67	9.88	7.51	8.30	13.04	9.49	9.09
Panel B FDR threshold	$\theta = 0.3$	4	13.44	9.09	8.70	11.86	11.07	7.11	9.09	13.44	9.88	8.70
		5	12.65	9.49	8.70	11.07	9.88	7.51	8.70	13.44	9.09	8.30
		6	11.86	8.30	8.30	10.67	9.88	7.51	8.30	12.65	9.09	8.30
	$\theta = 0.4$	4	13.04	8.70	9.09	11.86	10.28	7.51	8.30	13.04	9.88	9.09
		5	12.25	8.30	8.30	11.07	10.67	7.51	8.30	12.65	9.09	8.70
		6	12.25	8.70	8.30	9.88	9.49	7.51	7.91	11.86	9.09	8.30
	$\theta = 0.5$	4	12.65	9.09	8.30	11.07	11.07	7.51	9.09	12.25	9.09	9.09
		5	11.46	7.91	8.70	10.67	9.49	7.11	7.91	12.25	9.09	7.91
		6	11.07	7.91	8.30	10.28	9.49	6.72	7.91	12.25	9.09	8.30

This table reports the proportions of days with jumps identified by the PDS-based test for 10 NYSE stocks in 2020, with the control of spurious detections using (i) the universal threshold and (ii) the FDR threshold of Bajgrowicz et al. (2016). We use three pre-averaging windows $k_n = \lceil \theta\sqrt{N} \rceil$ with $\theta \in \{0.3, 0.4, 0.5\}$, different PDS barrier widths $c = K\sigma(\tilde{r}_i)$, i.e., the integer multiple of the standard deviation of pre-averaged returns, with K ranging from 4 to 6, and the censoring parameter $\epsilon = 0.05$. The total number of trading days is 253.

The adjusted results of our test for all selected stocks are reported in Table 7.[15] It is noteworthy that our testing results are fairly robust to the control of spurious detections, which underscores the empirical reliability of our PDS-based test.

6 Conclusions

This paper introduces a novel nonparametric high-frequency jump test for a discretely observed Itô semimartingale. Our approach utilizes a path-dependent sampling strategy for the tick-level price observations. The key intuition behind the construction of our test relies on the fact that, different from a continuous price increase or decrease over a certain time interval, a discontinuous shift with a larger magnitude will always trigger an exit-time event and induce a disproportionately large threshold exceedance under infill asymptotics. Additionally, a two-step noise reduction technique is designed to alleviate the impact of weakly dependent market microstructure noise. Through extensive simulations, we validate the reliable finite-sample performance of our test under empirically realistic specifications for price observations, which is convincingly superior to a comprehensive collection of "classical" methods. The Monte Carlo results demonstrate that the performance of our test is robust to various aggregation levels and tuning parameter choices. An empirical analysis

[15] See empirical results without and with the control of spurious detections for other calendar-time-sampling-based and noise-robust tests in Appendix B.3. Our test demonstrates somewhat similar performance to some noise-robust tests, but it stands out as the most robust to spurious detections, which further proves its reliability.

of NYSE-traded stocks provides strong statistical evidence for jumps across all selected stocks, and the results are robust to the correction of spurious detections. This methodology stands as the first exploration of the duration-based approach to test for jumps, which offers a robust and easy-to-implement tool for researchers and practitioners.

References

Aït-Sahalia, Y. and Jacod, J. (2009). Testing for jumps in a discretely observed process. *Annals of Statistics*, 37(1):184–222.

Aït-Sahalia, Y. and Jacod, J. (2014). *High-Frequency Financial Econometrics*. Princeton University Press.

Aït-Sahalia, Y., Jacod, J., and Li, J. (2012). Testing for jumps in noisy high frequency data. *Journal of Econometrics*, 168(2):207–222.

Aït-Sahalia, Y. and Kimmel, R. (2007). Maximum likelihood estimation of stochastic volatility models. *Journal of Financial Economics*, 83(2):413–452.

Aït-Sahalia, Y., Mykland, P. A., and Zhang, L. (2005). How often to sample a continuous-time process in the presence of market microstructure noise. *Review of Financial Studies*, 18(2):351–416.

Aït-Sahalia, Y., Mykland, P. A., and Zhang, L. (2011). Ultra high frequency volatility estimation with dependent microstructure noise. *Journal of Econometrics*, 160(1):160–175.

Andersen, T. G. and Bollerslev, T. (1997). Intraday periodicity and volatility persistence in financial markets. *Journal of Empirical Finance*, 4(2-3):115–158.

Andersen, T. G., Bollerslev, T., and Diebold, F. X. (2007a). Roughing it up: Including jump components in the measurement, modeling, and forecasting of return volatility. *Review of Economics and Statistics*, 89(4):701–720.

Andersen, T. G., Bollerslev, T., and Dobrev, D. (2007b). No-arbitrage semi-martingale restrictions for continuous-time volatility models subject to leverage effects, jumps and i.i.d. noise: Theory and testable distributional implications. *Journal of Econometrics*, 138(1):125–180.

Andersen, T. G., Bondarenko, O., Kyle, A. S., and Obizhaeva, A. A. (2018). Intraday trading invariance in the E-mini S&P 500 futures market. Working Paper.

Andersen, T. G., Dobrev, D., and Schaumburg, E. (2008). Duration-based volatility estimation. Working Paper.

Andersen, T. G., Dobrev, D., and Schaumburg, E. (2012). Jump-robust volatility estimation using nearest neighbor truncation. *Journal of Econometrics*, 169(1):75–93.

Andersen, T. G., Su, T., Todorov, V., and Zhang, Z. (2023). Intraday periodic volatility curves. *Journal of the American Statistical Association*, forthcoming.

Andersen, T. G., Thyrsgaard, M., and Todorov, V. (2019). Time-varying periodicity in intraday volatility. *Journal of the American Statistical Association*, 114(528):1695–1707.

Anscombe, F. J. (1952). Large-sample theory of sequential estimation. *Mathematical Proceedings of the Cambridge Philosophical Society*, 48(4):600–607.

Bajgrowicz, P., Scaillet, O., and Treccani, A. (2016). Jumps in high-frequency data: Spurious detections, dynamics, and news. *Management Science*, 62(8):2198–2217.

Bandi, F. M. and Russell, J. R. (2008). Microstructure noise, realized variance, and optimal sampling. *Review of Economic Studies*, 75(2):339–369.

Barndorff-Nielsen, O. E., Hansen, P. R., Lunde, A., and Shephard, N. (2009). Realized kernels in practice: Trades and quotes. *Econometrics Journal*, 12(3):1–32.

Barndorff-Nielsen, O. E. and Shephard, N. (2004). Power and bipower variation with stochastic volatility and jumps. *Journal of Financial Econometrics*, 2(1):1–37.

Barndorff-Nielsen, O. E. and Shephard, N. (2006). Econometrics of testing for jumps in financial economics using bipower variation. *Journal of Financial Econometrics*, 4(1):1–30.

Barndorff-Nielsen, O. E. and Shiryaev, A. N. (2015). *Change of Time and Change of Measure*. World Scientific Publishing.

Bibinger, M. and Winkelmann, L. (2015). Econometrics of co-jumps in high-frequency data with noise. *Journal of Econometrics*, 184(2):361–378.

Bollerslev, T., Li, J., and Liao, Z. (2021). Fixed-k inference for volatility. *Quantitative Economics*, 12(4):1053–1084.

Bollerslev, T., Li, S. Z., and Zhao, B. (2020). Good volatility, bad volatility, and the cross section of stock returns. *Journal of Financial and Quantitative Analysis*, 55(3):751–781.

Bollerslev, T., Todorov, V., and Xu, L. (2015). Tail risk premia and return predictability. *Journal of Financial Economics*, 118(1):113–134.

Borodin, A. N. and Salminen, P. (2002). *Handbook of Brownian Motion: Facts and Formulae*. Springer, Second edition.

Caporin, M., Kolokolov, A., and Renò, R. (2017). Systemic co-jumps. *Journal of Financial Economics*, 126(3):563–591.

Chernozhukov, V., Chetverikov, D., and Kato, K. (2013). Gaussian approximations and multiplier bootstrap for maxima of sums of high-dimensional random vectors. *Annals of Statistics*, 41(6):2786–2819.

Chernozhukov, V., Chetverikov, D., and Kato, K. (2019). Inference on causal and structural parameters using many moment inequalities. *Review of Economic Studies*, 86(5):1867–1900.

Christensen, K., Oomen, R., and Renò, R. (2022). The drift burst hypothesis. *Journal of Econometrics*, 227(2):461–497.

Corsi, F., Pirino, D., and Renò, R. (2010). Threshold bipower variation and the impact of jumps on volatility forecasting. *Journal of Econometrics*, 159(2):276–288.

Cremers, M., Halling, M., and Weinbaum, D. (2015). Aggregate jump and volatility risk in the cross-section of stock returns. *Journal of Finance*, 70(2):577–614.

Da, R. and Xiu, D. (2021). When moving-average models meet high-frequency data: Uniform inference on volatility. *Econometrica*, 89(6):2787–2825.

Dimitriadis, T. and Halbleib, R. (2022). Realized quantiles. *Journal of Business & Economic Statistics*, 40(3):1346–1361.

Dimitriadis, T., Halbleib, R., Polivka, J., Rennspies, J., Streicher, S., and Wolter, A. F. (2023). Efficient sampling for realized variance estimation in time-changed diffusion models. Working Paper.

Dumitru, A.-M. and Urga, G. (2012). Identifying jumps in financial assets: A comparison between nonparametric jump tests. *Journal of Business & Economic Statistics*, 30(2):242–255.

Durrett, R. (2019). *Probability: Theory and Examples*. Cambridge University Press, Fifth edition.

Engle, R. F. and Russell, J. R. (1998). Autoregressive conditional duration: A new model for irregularly spaced transaction data. *Econometrica*, 66(5):1127–1162.

Fan, J. and Yao, Q. (2003). *Nonlinear Time Series: Nonparametric and Parametric Methods*. Springer.

Fukasawa, M. and Rosenbaum, M. (2012). Central limit theorems for realized volatility under hitting times of an irregular grid. *Stochastic Processes and their Applications*, 122(12):3901–3920.

Gerhard, F. and Hautsch, N. (2002). Volatility estimation on the basis of price intensities. *Journal of Empirical Finance*, 9(1):57–89.

Gloter, A. and Jacod, J. (2001). Diffusions with measurement errors. I. Local asymptotic normality. *ESAIM: Probability and Statistics*, 5:225–242.

Gut, A. (2009). *Stopped Random Walks: Limit Theorems and Applications*. Springer, Second edition.

Gut, A. (2012). Anscombe's theorem 60 years later. *Sequential Analysis*, 31(3):368–396.

Hansen, P. R. and Lunde, A. (2006). Realized variance and market microstructure noise. *Journal of Business & Economic Statistics*, 24(2):127–161.

Harris, L. (1986). A transaction data study of weekly and intradaily patterns in stock returns. *Journal of Financial Economics*, 16(1):99–117.

Hautsch, N. and Podolskij, M. (2013). Preaveraging-based estimation of quadratic variation in the presence of noise and jumps: Theory, implementation, and empirical evidence. *Journal of Business & Economic Statistics*, 31(2):165–183.

Hong, S. Y., Nolte, I., Taylor, S. J., and Zhao, X. (2023). Volatility estimation and forecasts based on price durations. *Journal of Financial Econometrics*, 21(1):106–144.

Huang, X. and Tauchen, G. (2005). The relative contribution of jumps to total price variance. *Journal of Financial Econometrics*, 3(4):456–499.

Ibragimov, I. A. (1962). Some limit theorems for stationary processes. *Theory of Probability & Its Applications*, 7(4):349–382.

Ibragimov, I. A. and Linnik, Y. V. (1971). *Independent and Stationary Sequences of Random Variables*. Wolters-Noordhoff.

Jacod, J., Li, Y., Mykland, P. A., Podolskij, M., and Vetter, M. (2009). Microstructure noise in the continuous case: The pre-averaging approach. *Stochastic Processes and their Applications*, 119(7):2249–2276.

Jacod, J., Li, Y., and Zheng, X. (2017). Statistical properties of microstructure noise. *Econometrica*, 85(4):1133–1174.

Jacod, J., Li, Y., and Zheng, X. (2019). Estimating the integrated volatility with tick observations. *Journal of Econometrics*, 208(1):80–100.

Jiang, G. J. and Oomen, R. C. (2008). Testing for jumps when asset prices are observed with noise – a "swap variance" approach. *Journal of Econometrics*, 144(2):352–370.

Jiang, G. J. and Yao, T. (2013). Stock price jumps and cross-sectional return predictability. *Journal of Financial and Quantitative Analysis*, 48(5):1519–1544.

Kalnina, I. and Linton, O. (2008). Estimating quadratic variation consistently in the presence of endogenous and diurnal measurement error. *Journal of Econometrics*, 147(1):47–59.

Khaniyev, T. and Kucuk, Z. (2004). Asymptotic expansions for the moments of the Gaussian random walk with two barriers. *Statistics & Probability Letters*, 69(1):91–103.

Kolokolov, A. and Renò, R. (2024). Jumps or staleness? *Journal of Business & Economic Statistics*, 24(2):516–532.

Laurent, S. and Shi, S. (2020). Volatility estimation and jump detection for drift-diffusion processes. *Journal of Econometrics*, 217(2):259–290.

Lee, S. S. and Mykland, P. A. (2008). Jumps in financial markets: a new nonparametric test and jump dynamics. *Review of Financial Studies*, 21(6):2535–2563.

Lee, S. S. and Mykland, P. A. (2012). Jumps in equilibrium prices and market microstructure noise. *Journal of Econometrics*, 168(2):396–406.

Li, Y., Mykland, P. A., Renault, E., Zhang, L., and Zheng, X. (2014). Realized volatility when sampling times are possibly endogenous. *Econometric Theory*, 30(3):580–605.

Li, Z. M., Laeven, R. J., and Vellekoop, M. H. (2020). Dependent microstructure noise and integrated volatility estimation from high-frequency data. *Journal of Econometrics*, 215(2):536–558.

Li, Z. M. and Linton, O. (2022). A ReMeDI for microstructure noise. *Econometrica*, 90(1):367–389.

Liu, L. Y., Patton, A. J., and Sheppard, K. (2015). Does anything beat 5-minute RV? a comparison of realized measures across multiple asset classes. *Journal of Econometrics*, 187(1):293–311.

Lorden, G. (1970). On excess over the boundary. *Annals of Mathematical Statistics*, 41(2):520–527.

Lotov, V. I. (1996). On some boundary crossing problems for Gaussian random walks. *Annals of Probability*, 24(4):2154–2171.

Mancini, C. (2009). Non-parametric threshold estimation for models with stochastic diffusion coefficient and jumps. *Scandinavian Journal of Statistics*, 36(2):270–296.

Maneesoonthorn, W., Martin, G. M., and Forbes, C. S. (2020). High-frequency jump tests: Which test should we use? *Journal of Econometrics*, 219(2):478–487.

Nolte, I. and Xu, Q. (2015). The economic value of volatility timing with realized jumps. *Journal of Empirical Finance*, 34:45–59.

Pelger, M. (2020). Understanding systematic risk: A high-frequency approach. *Journal of Finance*, 75(4):2179–2220.

Podolskij, M. and Ziggel, D. (2010). New tests for jumps in semimartingale models. *Statistical Inference for Stochastic Processes*, 13(1):15–41.

Reiß, M. (2011). Asymptotic equivalence for inference on the volatility from noisy observations. *Annals of Statistics*, 39(2):772–802.

Rényi, A. (1957). On the asymptotic distribution of the sum of a random number of independent random variables. *Acta Mathematica Academiae Scientiarum Hungarica*, 8:193–199.

Rogozin, B. A. (1964). On the distribution of the first jump. *Theory of Probability & Its Applications*, 9(3):450–465.

Theodosiou, M. and Žikeš, F. (2011). A comprehensive comparison of alternative tests for jumps in asset prices. Working Paper.

Tse, Y.-K. and Yang, T. T. (2012). Estimation of high-frequency volatility: An autoregressive conditional duration approach. *Journal of Business & Economic Statistics*, 30(4):533–545.

Ubukata, M. and Oya, K. (2009). Estimation and testing for dependence in market microstructure noise. *Journal of Financial Econometrics*, 7(2):106–151.

Varneskov, R. T. (2017). Estimating the quadratic variation spectrum of noisy asset prices using generalized flat-top realized kernels. *Econometric Theory*, 33(6):1457–1501.

Vetter, M. and Zwingmann, T. (2017). A note on central limit theorems for quadratic variation in case of endogenous observation times. *Electronic Journal of Statistics*, 11(1):963–980.

Wood, R. A., McInish, T. H., and Ord, J. K. (1985). An investigation of transactions data for NYSE stocks. *Journal of Finance*, 40(3):723–739.

Wu, C.-F. J. (1986). Jackknife, bootstrap and other resampling methods in regression analysis. *Annals of Statistics*, 14(4):1261–1295.

Xiu, D. (2010). Quasi-maximum likelihood estimation of volatility with high frequency data. *Journal of Econometrics*, 159(1):235–250.

Yan, S. (2011). Jump risk, stock returns, and slope of implied volatility smile. *Journal of Financial Economics*, 99(1):216–233.

Zhang, L., Mykland, P. A., and Aït-Sahalia, Y. (2005). A tale of two time scales: Determining integrated volatility with noisy high-frequency data. *Journal of the American Statistical Association*, 100(472):1394–1411.

Zhou, B. (1996). High-frequency data and volatility in foreign-exchange rates. *Journal of Business & Economic Statistics*, 14(1):45–52.

Appendix A Proofs of Theorems and Propositions

A.1 Proof of Theorem 1 and 2

Proof. Firstly, we demonstrate that the difference between the limiting behavior of functionals of squared normalized PDS returns $|r_i^{(c)}/c|^2$ (i) under Assumption 2 and (ii) under the time-changed regular observation scheme in Remark 4 becomes negligible under infill asymptotics.

In all the sequel, the positive constants K and K' varies from line to line, but never depends on n, N, and $N^{(c)}$, and the various indices i, j. Unless specifically stated, we assume $X(\omega)$ is continuous, i.e., $\omega \in \Omega'$. Similar to the Assumption (S-HON) of Jacod et al. (2019), we impose the following stronger assumption without loss of generality by a classical localization procedure:

Assumption A.1. We have Assumptions 1 and 2 with $\tau_1 = \infty$. Moreover, the function δ and the processes μ, σ, λ, X are bounded, and we have $N \leq K\Delta_n^{-1}$ and $\mathbb{E}[\Delta_{n,i}^p] \leq K'\Delta_n^p$.

A.1.1 Intrinsic time. With an absolutely continuous time change from the calendar time t to intrinsic time $\tau(t)$:

$$t \to \tau(t) = \int_0^t \sigma_s^2 ds, \tag{A.1}$$

the intrinsic-time counterpart of X adapted to $(\mathcal{F}_t)_{t\geq 0}$ is

$$\widetilde{X}_{\tau(t)} = \widetilde{X}_0 + \int_0^{\tau(t)} \widetilde{\mu}_s ds + \widetilde{W}_{\tau(t)}, \tag{A.2}$$

where $\widetilde{\mu}$ is time-changed processes corresponding to μ in Eq. (1), and $\widetilde{W} = (\widetilde{W}_\tau)_{\tau\geq 0}$ is a Brownian motion evolving in intrinsic time. The relation $\widetilde{X}_{\tau(t)} = X_t$ holds for all t, and the τ-time process $\widetilde{X} = (\widetilde{X}_{\tau(t)})_{t\geq 0}$ is adapted to $(\widetilde{\mathcal{F}}_{\tau(t)})_{t\geq 0}$ with the τ-time σ-algebra satisfying $\widetilde{\mathcal{F}}_{\tau(t)} = \mathcal{F}_t$ (Lemma 1.2, Barndorff-Nielsen and Shiryaev, 2015). Particularly, when X is a calendar-time local martingale, $\widetilde{X}$ is an intrinsic-time Brownian motion (with an initial condition), which is implied by the Dambis-Dubins-Schwarz theorem. To simplify our discussions and avoid unnecessary complications, we assume the drift coefficient $\mu = 0$, which does not affect our asymptotic results.

A.1.2 Observation schemes. We start with two sequences of observations of $X(\omega)$:

(I) Under Assumption 2: X_{t_i}, for all $i = 0, 1, 2, \ldots, N$,
(II) Equidistant observations in intrinsic time: $\widetilde{X}_{i\Delta_n}$, for all $i = 0, 1, 2, \ldots, N$.

For the ease of notation, we denote $t_i \equiv t_{n,i}$ under Assumption 2, and $\breve{t}_i \equiv \tau^{-1}(i\Delta_n)$. The increments between successive observations are denoted by

$$r_i = X_{t_i} - X_{t_{i-1}} \qquad \text{and} \qquad \breve{r}_i = X_{\breve{t}_i} - X_{\breve{t}_{i-1}}, \tag{A.3}$$

for all $i \in \{1, 2, \ldots, N\}$. Lemma A.1 of Jacod et al. (2017) indicates the sequence (I) is an $(\mathcal{F}_t^n)$-martingale with Gaussian increments. Different from the independent but not identically distributed increments r_i, the increments $\breve{r}_i$ are i.i.d. normal with zero mean and variance Δ_n, which make the sequence (II) a homogenous Gaussian random walk.

Remark A.1. We assume both sequences have the same number $N \equiv N_1^n$ of observations. Assumption A.1 and Eq. (6) indicate that $T = \tau^{-1}(N\Delta_n)$ is bounded and $T \xrightarrow{\mathbb{P}} 1$ as $n \to \infty$. Moreover, by the triangle inequality and law of iterated expectations, Assumption 2 further implies $\mathbb{E}[|N\Delta_n - \tau(1)|] \leq K\Delta_n$, hence $|T - 1| = O_p(\Delta_n)$. That being said, the probability of jump occurrence in the "differenced part" of observation interval is negligible, see more discussions in Section 2.3 of Aït-Sahalia and Jacod (2009). To fix ideas, let $\delta \to 0$, then $\mathbb{P}(X_t'' \neq 0 \text{ for some } t \in [0, T] \triangle [0, 1]) \leq \mathbb{P}(|T-1| > \delta) + \mathbb{P}(X_t'' \neq 0 \text{ for some } t \in [1-\delta, 1+\delta]) = o(1)$, since we only assume potential jumps in $(0, 1)$.

For each sequence of observations, we conduct the PDS with the barrier width $c = m\sqrt{\Delta_n}$. We denote the squared PDS returns from each sequence of sampled observations by

$$\begin{aligned} R_i &= (r_i^{(c)})^2, \quad i \in \{1, 2, ..., N^{(c)}\}, \\ \breve{R}_i &= (\breve{r}_i^{(c)})^2, \quad i \in \{1, 2, ..., \breve{N}^{(c)}\}. \end{aligned} \tag{A.4}$$

Note that the PDS returns $\breve{r}_i^{(c)}$ are i.i.d., as implied by the strong Markov property of the Gaussian random walk (II) and the symmetric feature of the stopping rule in Eq. (9).

A.1.3 Some lemmas. We define two supremum processes $(Y_j)_{1 \leq j \leq N}$ and $(\breve{Y}_j)_{1 \leq j \leq N}$ as

$$Y_j = \sup_{1 \leq i \leq j} |X_{t_i}| \qquad \text{and} \qquad \breve{Y}_j = \sup_{1 \leq i \leq j} |X_{\breve{t}_i}|. \tag{A.5}$$

Lemma A.1. For any fixed $1 \leq j \leq N$, it holds for the supremum processes that

$$|Y_j - \breve{Y}_j| = O_p(j^2 \Delta_n^{1+\kappa/2} \sqrt{L_n}), \tag{A.6}$$

where for the ease of notation, $L_n \equiv \log N \asymp \log(\Delta_n^{-1})$.

Proof. Let $\mathcal{D}_n \equiv \sigma(\Delta_{n,1}, \Delta_{n,2}, \ldots)$ denote the σ-algebra generated by observation times. Note that by the triangle inequality of ℓ_∞-norm

$$\begin{aligned} |Y_j - \breve{Y}_j| &= \left| \max_{1 \leq i \leq j} |X_{t_i}| - \max_{1 \leq i \leq j} |X_{\breve{t}_i}| \right| \\ &\leq \max_{1 \leq i \leq j} |X_{t_i} - X_{\breve{t}_i}|. \end{aligned} \tag{A.7}$$

Note that by definition, we have with probability approaching 1,

$$\begin{aligned} X_{t_i} - X_{\check{t}_i} &= \sum_{\ell=1}^{i} \left(\int_{t_{\ell-1}}^{t_\ell} \sigma_s dW_s - \int_{\check{t}_{\ell-1}}^{\check{t}_\ell} \sigma_s dW_s \right) \\ &= \sum_{\ell=1}^{i} \left(\sigma_{t_{\ell-1}} (W_{t_\ell} - W_{t_{\ell-1}}) - \sigma_{\check{t}_{\ell-1}} (W_{\check{t}_\ell} - W_{\check{t}_{\ell-1}}) \right) \\ &+ \sum_{\ell=1}^{i} \left(\int_{t_{\ell-1}}^{t_\ell} (\sigma_s - \sigma_{t_{\ell-1}}) dW_s - \int_{\check{t}_{\ell-1}}^{\check{t}_\ell} (\sigma_s - \sigma_{\check{t}_{\ell-1}}) dW_s \right) \\ &\equiv A_{n,i}^{(1)} + A_{n,i}^{(2)}. \end{aligned} \tag{A.8}$$

For the first term, by the maximal inequality of Gaussian variables, we have

$$\mathbb{E}\Big[\max_{1 \le i \le j} |A_{n,i}^{(1)}| \Big| \mathcal{D}_n \Big] \le K \sqrt{ L_n \max_{1 \le i \le j} \Big| \sum_{\ell=1}^{i} (\Delta_{n,\ell} \lambda_{t_{\ell-1}} - \Delta_n) \Big| }. \tag{A.9}$$

For the right hand side, note that by the triangle inequality and Assumption 2 (ii),

$$\max_{1 \le i \le j} \Big| \sum_{\ell=1}^{i} \mathbb{E}\big[|\Delta_{n,\ell} \lambda_{t_{\ell-1}} - \Delta_n| \big| \mathcal{F}_{\ell-1}^n \big] \Big| \le K j \Delta_n^{2+\kappa}. \tag{A.10}$$

Combining Eq. (A.9) and Eq. (A.10), it follows the law of iterated expectation that

$$\max_{1 \le i \le j} |A_{n,i}^{(1)}| = O_p(j \Delta_n^{1+\kappa/2} \sqrt{L_n}). \tag{A.11}$$

For the second term in Eq. (A.8), by the maximal inequality, we have

$$\mathbb{E}\Big[\max_{1 \le i \le j} |A_{n,i}^{(2)}| \Big] \le K j \max_{1 \le i \le j} \mathbb{E}[|A_{n,i}^{(2)}|] \le K j^2 \Delta_n^{3/2+\kappa/2}, \tag{A.12}$$

where the last step is by the Burkholder-Davis-Gundy inequality and smoothness of σ regulated by Assumption 1 (iii). The proof of required statement is completed by the triangle inequality and Eqs. (A.7), (A.8), (A.11) and (A.12).

□

We define the first sampled observations for both sequences:

$$X_1^{(c)} = X_{\Pi_1^{(c)}} \qquad \text{and} \qquad \check{X}_1^{(c)} = \widetilde{X}_{\check{\Pi}_1^{(c)} \Delta_n}, \tag{A.13}$$

which means that the $\Pi_1^{(c)}$-th and the $\check{\Pi}_1^{(c)}$-th observations in (I) and (II), respectively, are the first to breach the symmetric double barrier. Lemma A.2 indicates that the first exit times of both sequences coincide with probability approaching 1 under infill asymptotics.

Lemma A.2. For $c = m\sqrt{\Delta_n}$, let $\overline{N}^{(c)} \equiv N^{(c)} \wedge \breve{N}^{(c)}$.

(i) For all integer $p \geq 1$, $\mathbb{E}[(\breve{\Pi}_1^{(c)})^p] < \infty$.

(ii) The first exit times for both sequences (I) and (II) satisfy

$$\mathbb{P}\Big(\max_{1 \leq i \leq \overline{N}^{(c)}} |\Pi_i^{(c)} - \breve{\Pi}_i^{(c)}| \geq 1 \Big) \leq K \Delta_n^{\kappa/2} \sqrt{L_n}. \tag{A.14}$$

Proof. (i) Note that $\breve{\Pi}_1^{(c)}$ has the same distribution as the number of steps for a standard Gaussian random walk $(Z_i)_{i=1,2,\ldots}$ to exit the double barrier $(-m, m)$. Let $h = \inf\{\tau : \widetilde{W}_\tau \notin (-m, m)\}$ denote the first exit time of the time-changed Brownian motion $\widetilde{W}$ from $(-m, m)$, then it is clear that $\breve{\Pi}_1^{(c)} - 1 \leq h$ by the continuity of Brownian motion, thus $\mathbb{E}[(\breve{\Pi}_1^{(c)} - 1)^p] \leq \mathbb{E}[h^p]$ for all $p > 0$. The Laplace transform of h is well-known in the literature, see, e.g., Eq. (3.0.1) in Borodin and Salminen (2002): $\mathbb{E}[e^{-\lambda h}] = \cosh^{-1} \sqrt{2\lambda} m$, and its Maclaurin series implies that $\mathbb{E}[h^p] < \infty$ for all integer $p \geq 1$. This completes the proof.

(ii) We start from the first term. By definition, we have

$$\mathbb{P}(\Pi_1^{(c)} \geq k) = \mathbb{P}(Y_k \leq c) \quad \text{and} \quad \mathbb{P}(\breve{\Pi}_1^{(c)} \geq k) = \mathbb{P}(\breve{Y}_k \leq c). \tag{A.15}$$

Let $\epsilon > 0$ be a positive number that can be arbitrarily small but not depend on N, it follows Lemma A.1 and the Markov inequality that

$$\begin{aligned}
\mathbb{P}(\Pi_1^{(c)} - \breve{\Pi}_1^{(c)} \geq 1) &= \sum_{k=1}^{N} \mathbb{P}(\breve{\Pi}_1^{(c)} = k) \mathbb{P}(\Pi_1^{(c)} > k | \breve{\Pi}_1^{(c)} = k) \\
&\leq \sum_{k=1}^{N} \mathbb{P}(\breve{\Pi}_1^{(c)} = k) \mathbb{P}(\breve{Y}_k - Y_k > \epsilon) \\
&\leq K \Delta_n^{1+\kappa/2} \sqrt{L_n} \Big[\sum_{k=1}^{N} k^2 \mathbb{P}(\breve{\Pi}_1^{(c)} = k) \Big] \\
&\leq K \Delta_n^{1+\kappa/2} \sqrt{L_n},
\end{aligned} \tag{A.16}$$

where the last line uses $\sum_{k=1}^{N} k^2 \mathbb{P}(\breve{\Pi}_1^{(c)} = k) \leq \mathbb{E}[(\breve{\Pi}_1^{(c)})^2] \leq K$ by Lemma A.2 (i). Similarly, we can also show

$$\mathbb{P}(\breve{\Pi}_1^{(c)} - \Pi_1^{(c)} \geq 1) \leq K \Delta_n^{1+\kappa/2} \sqrt{L_n}. \tag{A.17}$$

Combining above results, we have

$$\mathbb{P}(|\Pi_1^{(c)} - \breve{\Pi}_1^{(c)}| \geq 1) \leq K \Delta_n^{1+\kappa/2} \sqrt{L_n}. \tag{A.18}$$

Now, note that for any $2 \le q \le \overline{N}^{(c)}$, we have

$$\begin{aligned}\mathbb{P}\Big(\max_{1\le i\le q}|\Pi_i^{(c)}-\breve{\Pi}_i^{(c)}|\ge 1\Big) \le{}& \mathbb{P}\Big(\max_{1\le i\le q-1}|\Pi_i^{(c)}-\breve{\Pi}_i^{(c)}|\ge 1\Big)\\ &+\mathbb{P}\big(|\Pi_q^{(c)}-\breve{\Pi}_q^{(c)}|\ge 1\big|\Pi_i^{(c)}=\breve{\Pi}_i^{(c)} \text{ for all } 1\le i\le q-1\big).\end{aligned} \tag{A.19}$$

By the renewal property, we have $\Pi_q^{(c)}-\breve{\Pi}_q^{(c)} \overset{\mathcal{L}}{=} \Pi_1^{(c)}-\breve{\Pi}_1^{(c)}$ conditional on $\Pi_i^{(c)}=\breve{\Pi}_i^{(c)}$ for all $1\le i\le q-1$. Therefore, using a same argument as in driving Eq. (A.18), we can show the second term is bounded by $K\Delta_n^{1+\kappa/2}\sqrt{L_n}$. Applying the above argument recursively, we have

$$\begin{aligned}\mathbb{P}\Big(\max_{1\le i\le \overline{N}^{(c)}}|\Pi_i^{(c)}-\breve{\Pi}_i^{(c)}|\ge 1\Big) &\le K\overline{N}^{(c)}\Delta_n^{1+\kappa/2}\sqrt{L_n}\\ &\le K\Delta_n^{\kappa/2}\sqrt{L_n},\end{aligned} \tag{A.20}$$

for which we use $\overline{N}^{(c)} \asymp \Delta_n^{-1}$. The proof is then completed. □

Lemma A.3. Strong approximation for sampled return, it holds that

$$\mathbb{P}\Big(\max_{1\le i\le \overline{N}^{(c)}}|r_i^{(c)}-\breve{r}_i^{(c)}|>K\Delta_n^{1+\kappa/8}\Big)\le K'\Delta_n^{\kappa/8}\sqrt{L_n}. \tag{A.21}$$

Proof. It follows the maximal inequality of Gaussian variables that

$$\mathbb{E}\Big[\max_{1\le i\le N}|r_i-\breve{r}_i|\Big|\mathcal{D}_n\Big]\le K\sqrt{L_n}\max_{1\le i\le N}\sqrt{\big|\mathbb{E}[\Delta_{n,i}\lambda_{t_{i-1}}|\mathcal{F}_{i-1}^n]-\Delta_n\big|}\le K\Delta_n^{1+\kappa/2}\sqrt{L_n}. \tag{A.22}$$

Let $E_n\equiv\{\Pi_i^{(c)}=\breve{\Pi}_i^{(c)} \text{ for all } 1\le i\le N^{(c)}=\breve{N}^{(c)}\}$, we have $\mathbb{P}(E_n^{\complement})\le K\Delta_n^{\kappa/2}\sqrt{L_n}$ by Lemma A.2 (ii). Note that by the maximal inequality, we have for any $p>1$,

$$\mathbb{E}\Big[\max_{1\le i\le \breve{N}^{(c)}}|\breve{\Pi}_i^{(c)}-\breve{\Pi}_{i-1}^{(c)}|^p\Big]\le \breve{N}^{(c)}\max_{1\le i\le \breve{N}^{(c)}}\mathbb{E}[|\breve{\Pi}_i^{(c)}-\breve{\Pi}_{i-1}^{(c)}|^p]\le K_p\Delta_n^{-1}, \tag{A.23}$$

where the last step is by Lemma A.2 (i). Taking $p>4/\kappa$ gives

$$\mathbb{E}\Big[\max_{1\le i\le \breve{N}^{(c)}}|\breve{\Pi}_i^{(c)}-\breve{\Pi}_{i-1}^{(c)}|^2\Big]\le K\Delta_n^{-\kappa/2}. \tag{A.24}$$

Moreover, by Cauchy-Schwarz inequality, we obtain

$$\begin{aligned}\mathbb{E}\Big[\max_{1\le i\le \breve{N}^{(c)}}|r_i^{(c)}-\breve{r}_i^{(c)}|\Big|E_n\Big] &\le \sqrt{\mathbb{E}\Big[\max_{1\le i\le \breve{N}^{(c)}}|\breve{\Pi}_i^{(c)}-\breve{\Pi}_{i-1}^{(c)}|^2\Big]\mathbb{E}\Big[\max_{1\le \ell\le n}|r_\ell-\breve{r}_\ell|^2\Big]}\\ &\le K\Delta_n^{1+\kappa/4}\sqrt{L_n}.\end{aligned} \tag{A.25}$$

Therefore, we have

$$\begin{aligned}
&\mathbb{P}\Big(\max_{1\le i\le \overline{N}^{(c)}} |r_i^{(c)} - \breve{r}_i^{(c)}| > K\Delta_n^{1+\kappa/8}\Big) \\
&\le \mathbb{P}\Big(\max_{1\le i\le \breve{N}^{(c)}} |r_i^{(c)} - \breve{r}_i^{(c)}| > K\Delta_n^{1+\kappa/8}\Big| E_n\Big) + \mathbb{P}(E_n^{\complement}) \\
&\le K'(\Delta_n^{\kappa/8}\sqrt{L_n} + \Delta_n^{\kappa/2}\sqrt{L_n}).
\end{aligned} \tag{A.26}$$

This completes the proof.

□

Lemma A.3 shows the statistics constructed from sampled returns under observation schemes (I) and (II) are equivalent up to a $\Delta_n^{-1-\kappa/8}$ normalization, which is sufficient for the $c^{-1} \asymp \Delta_n^{-1/2}$ $\sqrt{\breve{N}^{(c)}} \asymp \Delta_n^{-1/2}$ order in conventional CLT. The requirement is only $\kappa > 0$.

The above type of strong approximation results are similarly used in, e.g., the proof of Theorem 5.1 in Chernozhukov et al. (2013) and the proof of Theorem 4.3 in Chernozhukov et al. (2019). It allows us to focus on the limiting behavior of functionals of $\breve{R}_i/c^2$, the result can be sufficiently extended to those of R_i/c^2. To fix ideas, consider a possibly multi-dimensional Lipschitz function $f(\cdot)$. Suppose that

$$\frac{1}{\breve{N}^{(c)}}\sum_{i=1}^{\breve{N}^{(c)}} f\Big(\frac{\breve{R}_i}{c^2}\Big) \xrightarrow{\mathbb{P}} \mu_f, \quad \text{and} \quad \frac{1}{\sqrt{\breve{N}^{(c)}}}\sum_{i=1}^{\breve{N}^{(c)}}\Big(f\Big(\frac{\breve{R}_i}{c^2}\Big) - \mu_f\Big) \xrightarrow{\mathcal{L}} \mathcal{N}(0, \Sigma_f). \tag{A.27}$$

Let $E_n' \equiv \{\Pi_i^{(c)} = \breve{\Pi}_i^{(c)} \text{ for all } 1 \le i \le \breve{N}^{(c)}\} \cap \{\max_{1\le i\le \breve{N}^{(c)}} |R_i - \breve{R}_i|/c^2 > K\Delta_n^{1/2+\kappa/16}\}$. Note that $a^2 - b^2 = (a-b)^2 + 2b(a-b)$, it follows triangle inequality that

$$\max_{1\le i\le \breve{N}^{(c)}} |R_i - \breve{R}_i| \le \Big(\max_{1\le i\le \breve{N}^{(c)}} |r_i^{(c)} - \breve{r}_i^{(c)}|\Big)^2 + 2\Big(\max_{1\le i\le \breve{N}^{(c)}} |\breve{r}_i^{(c)}|\Big)\Big(\max_{1\le i\le \breve{N}^{(c)}} |r_i^{(c)} - \breve{r}_i^{(c)}|\Big). \tag{A.28}$$

Note that $\max_{1\le i\le \breve{N}^{(c)}} |\breve{r}_i^{(c)}| = O_p(\Delta_n^{1/2}\sqrt{L_n}) = o_p(\Delta_n^{1/2-\kappa/16})$ by the maximal inequality of sub-Gaussian variables. Then it follows Lemma A.2 (ii), A.3, and Eq. (A.28) that $\mathbb{P}(E_n') \ge 1 - K\Delta_n^{\kappa/8}\sqrt{L_n}$. Therefore, for each $\varepsilon > 0$,

$$\begin{aligned}
&\mathbb{P}\Big(\Big\|\frac{1}{N^{(c)}}\sum_{i=1}^{N^{(c)}} f\Big(\frac{R_i}{c^2}\Big) - \mu_f\Big\| > \varepsilon\Big) \\
&\le \mathbb{P}\Big(\Big\|\frac{1}{\breve{N}^{(c)}}\sum_{i=1}^{\breve{N}^{(c)}} f\Big(\frac{\breve{R}_i}{c^2}\Big) - \mu_f\Big\| > \frac{\varepsilon}{2}\Big) + \mathbb{P}\Big(\Big\|\frac{1}{N^{(c)}}\sum_{i=1}^{N^{(c)}} f\Big(\frac{R_i}{c^2}\Big) - \frac{1}{\breve{N}^{(c)}}\sum_{i=1}^{\breve{N}^{(c)}} f\Big(\frac{\breve{R}_i}{c^2}\Big)\Big\| > \frac{\varepsilon}{2}\Big) \\
&\le \mathbb{P}\Big(\Big\|\frac{1}{\breve{N}^{(c)}}\sum_{i=1}^{\breve{N}^{(c)}} f\Big(\frac{\breve{R}_i}{c^2}\Big) - \mu_f\Big\| > \frac{\varepsilon}{2}\Big) + \mathbb{P}\Big(K\max_{1\le i\le \breve{N}^{(c)}}\frac{|R_i - \breve{R}_i|}{c^2} > \frac{\varepsilon}{2}\Big| E_n'\Big) + \mathbb{P}(E_n'^{\complement}) \\
&= \mathbb{P}\Big(\Big\|\frac{1}{\breve{N}^{(c)}}\sum_{i=1}^{\breve{N}^{(c)}} f\Big(\frac{\breve{R}_i}{c^2}\Big) - \mu_f\Big\| > \frac{\varepsilon}{2}\Big) + K\Delta_n^{\kappa/8}\sqrt{L_n}.
\end{aligned} \tag{A.29}$$

Let $Z \sim \mathcal{N}(0, \Sigma_f)$. For each $A \subset \mathbb{R}^{\dim(f)}$ and $\varepsilon > 0$, let $A^\varepsilon \equiv \{x \in \mathbb{R}^{\dim(f)} : \inf_{y \in A} \|x - y\| \leq \varepsilon\}$ denote the ε-enlargement of A, then we have

$$
\begin{aligned}
&\mathbb{P}\Big(\frac{1}{\sqrt{N^{(c)}}} \sum_{i=1}^{N^{(c)}} \Big(f\Big(\frac{R_i}{c^2}\Big) - \mu_f\Big) \in A\Big) \\
&\leq \mathbb{P}\Big(\frac{1}{\sqrt{\breve{N}^{(c)}}} \sum_{i=1}^{\breve{N}^{(c)}} \Big(f\Big(\frac{\breve{R}_i}{c^2}\Big) - \mu_f\Big) \in A^\varepsilon\Big) + \mathbb{P}\Big(\Big\|\frac{1}{\sqrt{N^{(c)}}} \sum_{i=1}^{N^{(c)}} f\Big(\frac{R_i}{c^2}\Big) - \frac{1}{\sqrt{\breve{N}^{(c)}}} \sum_{i=1}^{\breve{N}^{(c)}} f\Big(\frac{\breve{R}_i}{c^2}\Big)\Big\| > \varepsilon\Big) \\
&\leq \mathbb{P}\Big(\frac{1}{\sqrt{\breve{N}^{(c)}}} \sum_{i=1}^{\breve{N}^{(c)}} \Big(f\Big(\frac{\breve{R}_i}{c^2}\Big) - \mu_f\Big) \in A^\varepsilon\Big) + \mathbb{P}\Big(K\sqrt{\breve{N}^{(c)}} \max_{1 \leq i \leq \breve{N}^{(c)}} \frac{|R_i - \breve{R}_i|}{c^2} > \varepsilon \Big| E_n'\Big) + \mathbb{P}(E_n'^{\complement}) \\
&= \mathbb{P}(Z \in A) + \mathbb{P}(Z \in A^\varepsilon \setminus A) + K\Delta_n^{\kappa/8}\sqrt{L_n}.
\end{aligned}
\tag{A.30}
$$

Taking $\varepsilon \to 0$, the right-hand side becomes $\mathbb{P}(Z \in A) + o(1)$. Similarly, one can show

$$
\mathbb{P}\Big(\frac{1}{\sqrt{N^{(c)}}} \sum_{i=1}^{N^{(c)}} \Big(f\Big(\frac{R_i}{c^2}\Big) - \mu_f\Big) \in A\Big) \geq \mathbb{P}(Z \in A) - o(1). \tag{A.31}
$$

This shows the same CLT holds. Therefore, our attention is restricted to the limit theorems of the test statistics constructed from $(\breve{r}_i^{(c)})_{1 \leq i \leq \breve{N}^{(c)}}$. For ease of notation, we shall drop the breve mark ($\breve{}$) in the subsequent proofs.

A.1.4 Proof of Theorem 1.

Under the null. As randomly indexed partial sums of i.i.d. random variables, the PDS returns $r_i^{(c)}$ for all $1 \leq i \leq N^{(c)}$ form a stopped random walk. To consider the departure from ordinary limit theorems that hold for processes with fixed indices, some previous studies extend the standard results to accommodate randomly indexed random walks, see, e.g., Anscombe (1952), Rényi (1957), and Gut (2009, 2012).

Note that the condition specified in Anscombe's theorem (Theorem 1, Rényi, 1957; Theorem 2.2 and 2.3, Gut, 2012) is satisfied by the strong law for renewal processes, i.e., as $n \to \infty$,

$$
\frac{N^{(c)}}{N} \xrightarrow{\text{a.s.}} \mathbb{E}[\Pi_1^{(c)}] = \frac{1}{\mu_2(m)}, \tag{A.32}
$$

such that the random sum LLN implies, jointly with the continuous mapping theorem, that

$$
\frac{\sum_{i=1}^{N^{(c)}} R_i}{c^2 N^{(c)}} \xrightarrow{\mathbb{P}} h_2(m) \quad \text{and} \quad \frac{\sum_{i=1}^{N^{(c)}} \overline{R}_i}{c^2 N^{(c)}} \xrightarrow{\mathbb{P}} \overline{h}_{2,\epsilon}(m). \tag{A.33}
$$

The consistency of both $\overline{M}_{c,\epsilon}$ and M_c in Eq. (17) is a direct result of the continuous mapping theorem from Eq. (A.33).

Under the alternative. We denote by (Λ_t^n) the counting process of all jumps in (X_t^n) in Eq. (7), then Λ_t^n is bounded for each n, and for all n, we have

$$\sum_{0\le s\le t} |\Delta X_t^n|^r < \infty, \tag{A.34}$$

which implies for large enough n (such that $u_n \to 0$),

$$u_n^r \Lambda_t^n \le \sum_{0\le s\le t} |\Delta X_t^n|^r < \infty, \tag{A.35}$$

from which one can deduce that $\Lambda_t^n = O_p(\Delta_n^{-r/2})$ for all fixed t.

When $X(\omega)$ is discontinuous within $(0,1)$, we denote by $\{s_1, s_2 \ldots, s_\Lambda\}$ the sequence of all jump times in chronological order, where $\Lambda \equiv \Lambda_1^n(\omega)$ counts the number of all discontinuities on $(0,1]$. We define

$$k^-(s) = \inf_{0\le i\le n} \{t_i \ge s : |t_i - s|\} \quad \text{and} \quad k^+(s) = \inf_{0\le i\le n} \{t_i < s : |t_i - s|\} \tag{A.36}$$

as the index of the first observations no earlier than and strictly before s, respectively. We split the sequence of observations $(X_{t_i})_{0\le i\le N}$ into $\Lambda+1$ segments with $i = k^+(s_j)$ for all $1 \le j \le \Lambda$ as cutoff points. As $N \to \infty$, we have $k^+(s_j) - k^+(s_{j-1}) \to \infty$ (also, $k^+(s_1) \to \infty$), since any intervals of length of order Δ_n mostly contain a single jump of size larger than u_n, see Section 2.3 of Aït-Sahalia and Jacod (2009).

For each segment $(X_{t_i})_{k^+(s_{j-1})\le i\le k^+(s_j)}$, we obtain the PDS returns $(r_i^{(c)})_{N_{j-1}^{(c)}+1\le i\le N_j^{(c)}}$ with the barrier width $c = m\sqrt{\Delta_n}$. For each $i \in A_n = \{N_1^{(c)}, N_2^{(c)}, \ldots, N_\Lambda^{(c)}\}$, the PDS return $|r_i^{(c)}| \ge u \gg c$ contains jumps and will be censored by $\varphi_\epsilon(c)$. For all $i \notin A_n$, the PDS return $r_i^{(c)}$ contains only aggregated Brownian increments. For the censored PDS returns, we have

$$\frac{\sum_{i=1}^{N^{(c)}} \overline{R}_i}{c^2 N^{(c)}} = \frac{\sum_{i\notin A_n} \overline{R}_i}{c^2 N^{(c)}} + \frac{\sum_{i\in A_n} \overline{R}_i}{c^2 N^{(c)}}. \tag{A.37}$$

For the first term above, since the cardinality of A_n is $\Lambda = O_p(\Delta_n^{-r/2}) \ll \Delta_n^{-1} \asymp N^{(c)}$, we have

$$\frac{\sum_{i\notin A_n} \overline{R}_i}{c^2 N^{(c)}} = \frac{N^{(c)} - \Lambda}{N^{(c)}} \frac{\sum_{i\notin A_n} \overline{R}_i}{c^2 (N^{(c)} - \Lambda)}, \quad \text{where } \frac{N^{(c)} - \Lambda}{N^{(c)}} \xrightarrow{\text{a.s.}} 1, \tag{A.38}$$

such that it coincides with the limit theorems under the null. For the second term, it holds that

$$\frac{\sum_{i\in A_n} \overline{R}_i}{c^2 N^{(c)}} \le K \frac{\Lambda}{N^{(c)}} \le K' \Delta_n^{1-r/2}, \tag{A.39}$$

which has no impact on the LLN result. It still vanishes after multiplying by $\sqrt{N^{(c)}} \asymp \Delta_n^{-1/2}$ for any $r \in [0,1)$, and thus does not affect the CLT.

For uncensored PDS returns, it holds that as $n \to \infty$,

$$\frac{\sum_{i=1}^{N^{(c)}} R_i}{c^2 N^{(c)}} \xrightarrow{\mathbb{P}} \frac{h_2(m)[X,X]_1}{\tau(1)}, \quad \text{where } \tau(1) = \int_0^1 \sigma_s^2 ds, \tag{A.40}$$

because $\sum_{i=1}^{N^{(c)}} R_i \xrightarrow{\mathbb{P}} [X,X]_1$ and $c^2 N^{(c)} \xrightarrow{\mathbb{P}} \tau(1)/h_2(m)$. This completes the proof.

A.1.5 Proof of Theorem 2. As mentioned in Appendix A.1.4, the condition in Anscombe's theorem is satisfied. The random index version of Lindeberg-Lévy CLT (Theorem 2.3, Gut, 2012) can be applied to verify the asymptotic normality of $(\overline{M}_{c,\epsilon}, M_c)'$. We start with an i.i.d. two-dimensional random vector

$$X_i = \left(\frac{\overline{R}_i}{c^2}, \frac{R_i}{c^2}\right)', \tag{A.41}$$

with the mean vector

$$\mathbb{E}[X_i] \xrightarrow{\mathbb{P}} \mu = (\overline{h}_{2,\epsilon}(m), h_2(m))', \tag{A.42}$$

and a 2×2 variance-covariance matrix (among the components of the vector):

$$\mathrm{Var}(X_i) \xrightarrow{\mathbb{P}} \Sigma, \quad \text{where } \Sigma = m^{-4} \begin{bmatrix} \overline{\mu}_{4,\epsilon}(m) - \overline{\mu}_{2,\epsilon}^2(m) & \overline{\rho}_{2,\epsilon}(m) - \mu_2(m)\overline{\mu}_{2,\epsilon}(m) \\ \overline{\rho}_{2,\epsilon}(m) - \mu_2(m)\overline{\mu}_{2,\epsilon}(m) & \mu_4(m) - \mu_2^2(m) \end{bmatrix}. \tag{A.43}$$

The functions in Σ, i.e., μ, $\overline{\mu}$, and $\overline{\rho}$, are defined in Section 3.1.

For the sample mean vector

$$\overline{X} = \frac{1}{N^{(c)}} \sum_{i=1}^{N^{(c)}} X_i = \left(\frac{1}{N^{(c)}} \sum_{i=1}^{N^{(c)}} \frac{\overline{R}_i}{c^2}, \frac{1}{N^{(c)}} \sum_{i=1}^{N^{(c)}} \frac{R_i}{c^2}\right)' = (\overline{S}_{2,\epsilon}, S_2)', \tag{A.44}$$

where the summation of these vectors is being done component-wise. The random sum Lindeberg-Lévy CLT implies that as $n \to \infty$,

$$\sqrt{N^{(c)}}(\overline{X} - \mu) \xrightarrow{\mathcal{L}} \mathcal{N}(0, \Sigma), \tag{A.45}$$

and

$$\sqrt{N}(\overline{X} - \mu) \xrightarrow{\mathcal{L}} \mathcal{N}(0, \mu_2(m)\Sigma). \tag{A.46}$$

Therefore, for the random vector

$$f(\overline{X}) = (\overline{M}_{c,\epsilon}, M_c)', \tag{A.47}$$

with the vector function

$$f\left(\begin{bmatrix} x \\ y \end{bmatrix}\right) = \begin{bmatrix} \overline{h}_{2,\epsilon}^{-1}(x) \\ h_2^{-1}(y) \end{bmatrix}, \tag{A.48}$$

it holds that

$$\sqrt{N}(f(\overline{X}) - m) \xrightarrow{\mathcal{L}} \mathcal{N}(0,\ \mu_2(m) \triangledown f(\mu)' \Sigma \triangledown f(\mu)), \tag{A.49}$$

by the multivariate delta method, where

$$\nabla f(\mu) = ((\overline{h}'_{2,\epsilon}(\overline{h}^{-1}_{2,\epsilon}(\overline{h}_{2,\epsilon}(m))))^{-1}, (h_2'(h_2^{-1}(h_2^{-1}(m))))^{-1}) = ((\overline{h}'_{2,\epsilon}(m))^{-1}, (h_2'(m))^{-1}). \tag{A.50}$$

This completes the proof. □

A.2 Proof of Proposition 1

Proof. Firstly, we prove that the sequence of pre-averaged returns $(r_i^*)_{1\leq i\leq N'}$ converges in law to a centered stationary Gaussian process with desired variance under infill asymptotics for each i. We assume $k_n = 2k$ for simplicity, and expand r_i^* in terms of $\Delta_j^N X = X_j - X_{j-1}$ and ε_j:

$$\begin{aligned} r_i^* &= \frac{1}{k_n}\sum_{j=1}^{k}(X_{i+k+j} - X_{i+j}) + \frac{1}{k_n}\sum_{j=1}^{k}(\varepsilon_{i+k+j} - \varepsilon_{i+j}) \\ &= \underbrace{\sum_{j=1}^{k_n} g\Big(\frac{j}{2k}\Big)\Delta_{i+j}^N X}_{A_i} + \underbrace{\frac{1}{k_n}\sum_{j=1}^{k}(\varepsilon_{i+k+j} - \varepsilon_{i+j})}_{B_i}, \end{aligned} \tag{A.51}$$

where $g(s) = s \wedge (1-s)$ is the triangular kernel weighting function. Under Assumption 2 and by the strong approximation result in Eq. (A.22), we deduce that A_i converges in probability to $\sum_{j=1}^{k_n} g\big(\frac{j}{2k}\big)\breve{r}_{i+j}$, which is a linear combination of i.i.d. centered Gaussian random variables. The α-mixing ε with the conditions in Assumption 3 indidates a CLT under weak dependence (Ibragimov, 1962; Theorem 8.3.7, Durrett, 2019), which implies the asymptotic Gaussianity of B_i. The independence between X and ε implies that r_i^* converges in distribution to a centered Gaussian random variable for all i.

We now identify the limiting law of (r_i^*) by calculating its variance kernel explicitly, which also establishes the stationarity of the limiting Gaussian process. With $\mathrm{Corr}(X_j, \varepsilon_{j'}) = 0$ for any $0 \leq j, j' \leq N$, we have $\mathrm{Var}(r_i^*) = \mathrm{Var}(A_i) + \mathrm{Var}(B_i)$ with

$$\mathrm{Var}(A_i) = \sum_{j=1}^{k_n} g^2\Big(\frac{j}{k_n}\Big)(\Delta_n + o(\Delta_n)) = \frac{k_n\Delta_n}{12} + o(\sqrt{\Delta_n}). \tag{A.52}$$

For the additive noise term, we define the partial sum of ε as

$$S_{n,h} = \sum_{i=1}^{h}\varepsilon_{n+i}, \tag{A.53}$$

and start with the following results for some $\lambda \geq h$:

$$\mathrm{Var}(S_{n,h}) = \sum_{m=1-h}^{h-1}(h - |m|)\Gamma_m = h\sum_{m=1-h}^{h-1}\Big(1 - \Big|\frac{m}{h}\Big|\Big)\Gamma_m, \tag{A.54}$$

$$\begin{aligned}\mathrm{Cov}(S_{n,h}, S_{n+\lambda,h}) &= \mathbb{E}[S_{n,h}S_{n+\lambda,h}] = \sum_{i=0}^{h-1}\sum_{j=0}^{h-1}\mathrm{Cov}(\varepsilon_{n+i}, \varepsilon_{n+\lambda+i+j}) \\ &= \sum_{m=1-h}^{h-1}(h-|m|)\Gamma_{m+\lambda} = h\sum_{m=1-h}^{h-1}\Big(1-\Big|\frac{m}{h}\Big|\Big)\Gamma_{m+\lambda},\end{aligned} \tag{A.55}$$

where the weight $1-|m/h|$ is the Bartlett kernel. Therefore, we have

$$\begin{aligned}\mathrm{Var}(B_i) &= \frac{1}{4k^2}\mathrm{Var}(S_{i+k,k} - S_{i,k}) \\ &= \frac{1}{4k^2}\mathrm{Var}(S_{i+k,k}) + \frac{1}{4k^2}\mathrm{Var}(S_{i,k}) - 2\mathrm{Cov}(S_{i+k,k}, S_{i,k}) \\ &= \frac{1}{2k}\sum_{m=1-k}^{k-1}\Big(1-\Big|\frac{m}{k}\Big|\Big)\Gamma_m - \frac{1}{2k}\sum_{m=1-k}^{k-1}\Big(1-\Big|\frac{m}{k}\Big|\Big)\Gamma_{m+k}\end{aligned} \tag{A.56}$$

of the order $\sqrt{\Delta_n}$ by the absolute summability of Γ_m, which is implied by the α-mixing property of ε under Assumption 3 (Ibragimov and Linnik, 1971). Since $k_n \asymp \sqrt{N}$, both $\mathrm{Var}(A_i)$ and $\mathrm{Var}(B_i)$ are of the order $\sqrt{\Delta_n}$, such that we can ignore all terms with order smaller than $\sqrt{\Delta_n}$, which yields $\mathrm{Var}(r_i^*) = \mathrm{Var}(A_i) + \mathrm{Var}(B_i) \asymp \sqrt{\Delta_n}$.

With the time-invariant first moment and finite second moment of r_i^* for all time, in order to prove the weak stationarity of (r_i^*), we need to make sure that the autocovariance $\mathrm{Cov}(r_i^*, r_{i+\lambda}^*)$ does not vary with i. Here we firstly deal with the autocovariance of A_i. It suffices to examine the autocovariance for non-negative integer-valued lags λ, as the autocovariance function is always symmetric.

$$\mathrm{Cov}(A_i, A_{i+\lambda}) = \mathbb{E}[A_iA_{i+\lambda}] = \mathbb{E}\left[\sum_{j=1}^{k_n} g\Big(\frac{j}{k_n}\Big)\Delta_{i+j}^N X \sum_{\eta=1}^{k_n} g\Big(\frac{\eta}{k_n}\Big)\Delta_{i+\lambda+\eta}^N X\right]. \tag{A.57}$$

When $\lambda \geq k_n$, $\mathrm{Cov}(A_i, A_{i+\lambda}) = 0$. When $1 \leq \lambda \leq k_n - 1$, we have

$$\begin{aligned}\mathrm{Cov}(A_i, A_{i+\lambda}) &= \mathbb{E}\left[\sum_{j=1}^{k_n-\lambda} g\Big(\frac{j}{k_n}\Big)g\Big(\frac{j+\lambda}{k_n}\Big)(\Delta_{i+\lambda+j}^N X)^2\right] \\ &= \sum_{j=1}^{k_n-\lambda} g\Big(\frac{j}{k_n}\Big)g\Big(\frac{j+\lambda}{k_n}\Big)\mathbb{E}[(\Delta_{i+\lambda+j}^N X)^2] = O(\sqrt{\Delta_n}).\end{aligned} \tag{A.58}$$

For the noise term, we have the lag-λ autocovariance

$$\begin{aligned}
&\mathrm{Cov}(B_i, B_{i+\lambda}) = \frac{1}{4k^2}\mathbb{E}[(S_{i+k,k} - S_{i,k})(S_{i+k+\lambda,k} - S_{i+\lambda,k})] \\
&= \frac{1}{4k^2}\left(\mathbb{E}[S_{i+k,k}S_{i+k+\lambda,k}] + \mathbb{E}[S_{i,k}S_{i+\lambda,k}] - \mathbb{E}[S_{i+k,k}S_{i+\lambda,k}] - \mathbb{E}[S_{i,k}S_{i+k+\lambda,k}]\right) \\
&= \frac{1}{2k}\sum_{m=1-k}^{k-1}\left(1 - \left|\frac{m}{k}\right|\right)\Gamma_{m+\lambda} - \frac{1}{4k}\sum_{m=1-k}^{k-1}\left(1 - \left|\frac{m}{k}\right|\right)\Gamma_{m+\lambda-k} - \frac{1}{4k}\sum_{m=1-k}^{k-1}\left(1 - \left|\frac{m}{k}\right|\right)\Gamma_{m+\lambda+k} \\
&= O(\sqrt{\Delta_n}),
\end{aligned} \tag{A.59}$$

by the absolute summability of Γ_m. In the limit, both the covariances are finite and time-invariant (not depend on i) for all possible $\lambda \in \mathbb{N}$, which implies the weak stationarity of (r_i^*) in the limit, as desired.

For Step 2, we first demonstrate how the random sign flip eliminates serial correlations in (r_i^*). Let $F(x) = \mathbb{P}(r_i^* \le x)$ denote the CDF of r_i^*. It is obvious that the product $\delta_i r_i^*$ is a Gaussian random variable with the same distribution:

$$\begin{aligned}
\mathbb{P}(\delta_i r_i^* \le x) &= \mathbb{P}(\delta_i = 1)\mathbb{P}(\delta_i r_i^* \le x | \delta_i = 1) + \mathbb{P}(\delta_i = -1)\mathbb{P}(\delta_i r_i^* \le x | \delta_i = -1) \\
&= \frac{1}{2}\mathbb{P}(r_i^* \le x) + \frac{1}{2}\mathbb{P}(r_i^* \ge -x) = F(x),
\end{aligned} \tag{A.60}$$

and the autocovariance function for any $i \in \{1, \ldots, N' - \lambda\}$ satisfies

$$\mathrm{Cov}(\delta_i r_i^*, \delta_{i+\lambda} r_{i+\lambda}^*) = \mathbb{E}[\delta_i \delta_{i+\lambda} r_i^* r_{i+\lambda}^*] = \mathbb{E}[\delta_i]\mathbb{E}[\delta_{i+\lambda}]\mathrm{Cov}(r_i^*, r_{i+\lambda}^*) = 0. \tag{A.61}$$

Next, we establish that, following the uniform random permutation $\pi : \{1, \ldots, N'\} \mapsto \{1, \ldots, N'\}$, any two variables in $(\tilde{r}_i)_{1 \le i \le N'}$ are independent when their indices are not sufficiently distant from each other each other in $\{1, \ldots, N'\}$ under infill asymptotics. We start with a formal definition of the local independence for a discrete-time stochastic process: The process $X = (X_i)_{1 \le i \le n}$ is said to be locally independent if

$$\begin{aligned}
&\lim_{n\to\infty} \sup_{\substack{1 \le i,j \le n \\ 1 \le |i-j| \le \Lambda_n}} \mathbb{P}(X_i \text{ and } X_j \text{ are dependent}) = 0, \\
\text{or} \quad &\lim_{n\to\infty} \sup_{\substack{1 \le i,j \le n \\ 1 \le |i-j| \le \Lambda_n}} \{|\mathbb{P}(A \cap B) - \mathbb{P}(A)\mathbb{P}(B)| : A \in \sigma(X_i), B \in \sigma(X_j)\} = 0,
\end{aligned} \tag{A.62}$$

where $\Lambda_n \asymp n^{\varpi}$ for some $\varpi \in (0, 1)$, such that X_i is independent to other variables in X whose indices fall within the interval $[i - \Lambda_n, i + \Lambda_n]$. In our case, we need to verify

$$\lim_{n\to\infty} \sup_{\substack{1 \le i,j \le N' \\ 1 \le |i-j| \le \Lambda_n}} \mathbb{P}(\tilde{r}_i \text{ and } \tilde{r}_j \text{ are dependent}) = 0. \tag{A.63}$$

The fact that $(\varepsilon_i)_{0\le i\le N}$ is α-mixing implies that

$$\alpha(\Lambda_n) = \sup\{|\mathbb{P}(A\cap B) - \mathbb{P}(A)\mathbb{P}(B)| : A\in\sigma(\varepsilon_i), B\in\sigma(\varepsilon_{i+\Lambda_n})\} \to 0, \tag{A.64}$$

as $n\to\infty$, thus ε_i and ε_j are asymptotically independent if $|i-j|\ge\Lambda_n$.

With the uniform random permutation, we denote

$$\tilde{r}_i = r^*_{\pi(i)}\delta_{\pi(i)} \quad \text{and} \quad \tilde{r}_j = r^*_{\pi(j)}\delta_{\pi(j)} \tag{A.65}$$

where $\pi(i)$, $\pi(j)$ are the corresponding indices of the products before permutation. Therefore, for all $1\le i,j\le N'$ and $1\le|i-j|\le\Lambda_n$, $\tilde{r}_i$ and $\tilde{r}_j$ are independent if the corresponding indices $\pi(i)$ and $\pi(j)$ are sufficiently far apart from one another:

$$\begin{aligned}
\mathbb{P}(\tilde{r}_i \text{ and } \tilde{r}_j \text{ are dependent}) &= \mathbb{P}(r^*_{\pi(i)} \text{ and } r^*_{\pi(j)} \text{ are dependent})\\
&= \mathbb{P}(\sigma(\{\varepsilon_{\pi(i)+\ell} : 0\le\ell\le k_n\}) \text{ and } \sigma(\{\varepsilon_{\pi(j)+\ell} : 0\le\ell\le k_n\}) \text{ are dependent})\\
&\le 2\mathbb{P}(\pi(i)+1\le\pi(j)\le\pi(i)+k_n+\Lambda_n)\\
&= \frac{2(k_n+\Lambda_n)}{N'-1} = O(\Delta_n^{\gamma}), \quad \text{where } \gamma = 1-\max\Big\{\frac{1}{2},\varpi\Big\}.
\end{aligned} \tag{A.66}$$

For a sequence of N' variables, the uniform random permutation ensures that each of the $N'!$ possible permutations are equally likely and that each "ball" $r^*_{\pi(i)}\delta_{\pi(i)}$ has an equal chance of being placed into any "box" i, which has become a question of classical probability. As $n\to\infty$, $\tilde{r}_i$ and $\tilde{r}_j$ with $1\le|i-j|\le\Lambda_n$ are asymptotically independent. This completes the proof. □

Appendix B Supplementary Results

B.1 Parameter Choices for Other Tests

For other tests constructed in Sections 4 and 5, we clarify some specific parameter choices:

LM: For the local realized bipower variation, we consider the window size $K = \sqrt{252N}$, where N is the number of sampled observations.

ASJ: For the multipower variations constructed on two different sampling intervals δ and $k\delta$, we select $p = 4$ and $k = 2$, which satisfies the requirement.

CPR: For the auxiliary local variance estimator, we employ the nonparametric filter of length $2L + 1$ with $L = 25$ and a Gaussian kernel, which follows the recommendation in Appendix B of Corsi et al. (2010).

PZ: We employ the truncated realised power variation with $p = 4$ and the truncation threshold $cN^{-\varpi}$, where c and ϖ follow the recommendation in Section 5 of Podolskij and Ziggel (2010). For the noise-adjusted version, we select the pre-averaging window $k_n = 0.5\lfloor\sqrt{N}\rfloor$.

LM12: We select the pre-averaging window $k_n = 0.4\lfloor\sqrt{N}\rfloor$, which minimizes the absolute distance between the nominal size and the empirical size with the simulated tick-level noise-contaminated observations.

ASJL: We select the pre-averaging window $k_n = 0.9\lfloor\sqrt{N}\rfloor$ based on the simulated noise-contaminated data, and the truncation level $C = 5$.

B.2 Simulation Results with Other Noise Specifications

In addition to the simulation results in Section 4, we consider three other specifications for the additive noise that follows Aït-Sahalia et al. (2012) as robustness checks:

(i) Gaussian noise:

$$\varepsilon_i = 2Z_i\sqrt{\frac{\sigma^2_{t_{n,i}}}{n}}, \tag{B.1}$$

where Z_i are i.i.d. draws from a standard normal distribution, see Tables B.1 to B.3.

(ii) Autocorrelated Gaussian noise:

$$\varepsilon_i = 2\omega^A_i\sqrt{\frac{\sigma^2_{t_{n,i}}}{n}}, \tag{B.2}$$

where ω^A_i is an autocorrelated Gaussian defined in Eq. (31), see Tables B.4 to B.6.

(iii) t-distributed noise:

$$\varepsilon_i = 2\omega^B_i\sqrt{\frac{\nu-2}{\nu}}\sqrt{\frac{\sigma^2_{t_{n,i}}}{n}}, \tag{B.3}$$

where ω^B_i are i.i.d. draws from a Student's t distribution with the degree of freedom ν, see Tables B.7 to B.9.

Table B.1: Finite-sample size and power (%) under Gaussian noise

Nominal size: 5%		$\theta = 0.3$				$\theta = 0.4$				$\theta = 0.5$			
			ϵ				ϵ				ϵ		
	$c/\sigma(\tilde{r}_i)$	$N^{(c)}$	0.05	0.07	0.10	$N^{(c)}$	0.05	0.07	0.10	$N^{(c)}$	0.05	0.07	0.10
Panel A No Jump	3	1785	4.90	5.21	5.35	1783	5.07	5.05	5.76	1783	5.01	5.07	5.70
	4	1099	5.33	5.03	5.49	1098	4.93	5.14	5.81	1098	5.24	5.21	5.62
	5	743	4.71	5.14	5.33	743	5.18	5.28	5.43	742	5.10	5.70	5.27
	6	535	5.26	5.01	5.49	535	4.63	4.89	5.53	535	4.82	5.47	5.13
	7	404	4.71	4.99	5.19	404	4.61	5.55	5.62	404	5.17	5.18	5.08
	8	316	4.83	4.79	5.59	315	4.83	5.23	5.73	315	5.08	5.12	5.30
	9	254	5.44	4.80	5.30	253	5.22	5.00	5.38	253	5.20	5.20	5.73
	10	208	4.93	5.31	5.71	208	4.98	5.41	5.68	208	5.18	5.28	5.75
Panel B Moderate Jump	3	1715	47.74	49.52	50.82	1716	44.73	47.04	49.52	1718	42.85	45.35	47.45
	4	1058	46.68	48.74	50.80	1059	43.38	46.51	48.46	1061	41.71	44.74	46.93
	5	717	45.27	47.51	50.26	718	43.27	45.29	48.09	720	41.23	43.10	45.95
	6	518	44.45	47.15	49.63	519	43.24	44.57	46.91	520	41.10	42.06	45.13
	7	392	44.91	46.79	49.45	393	42.51	43.70	46.51	394	40.31	41.96	44.21
	8	307	42.82	46.95	49.09	308	41.76	43.10	45.84	308	39.45	40.95	44.10
	9	247	42.13	45.59	48.45	248	40.81	42.65	46.06	248	38.43	40.97	43.46
	10	203	41.42	44.81	48.32	204	40.32	41.82	46.46	204	38.26	40.44	43.70
Panel C Large Jump	3	1587	69.98	71.41	73.31	1589	68.18	69.74	71.08	1594	67.26	68.39	69.95
	4	979	68.91	71.10	72.74	982	67.81	69.39	70.89	985	65.92	67.49	69.41
	5	665	68.80	70.14	72.20	668	66.75	69.09	70.32	670	65.28	66.87	69.25
	6	482	67.64	69.69	71.54	485	66.71	68.34	69.77	487	64.99	66.15	68.20
	7	365	67.61	69.10	71.27	368	65.47	66.78	69.89	370	63.94	65.80	67.99
	8	287	67.37	68.95	71.00	289	65.11	66.62	68.93	291	64.21	65.45	66.91
	9	232	65.90	69.22	70.84	234	64.78	66.60	68.88	235	63.87	64.83	67.73
	10	191	65.47	68.02	70.71	193	64.23	65.74	68.45	194	63.14	64.76	67.56

This table reports the finite-sample size and size-adjusted power (%) of 10,000 simulations of the test statistic $T_{c,\epsilon}$ at 5% nominal level. All simulated prices are contaminated by the additive Gaussian mixture noise and rounding errors. We utilize the two-step noise reduction method in Section 3.2 to construct the sequence of pseudo-observations with three different pre-averaging windows, i.e., $k_n = \lceil \theta\sqrt{N} \rceil$ with $\theta \in \{0.3, 0.4, 0.5\}$. The observations are sampled with different PDS barrier widths $c = K\sigma(\tilde{r}_i)$, where K ranges from 3 to 10. Different censoring thresholds with $\epsilon \in \{0.05, 0.07, 0.1\}$ are considered. $N^{(c)}$ stands for the average sampling frequencies.

Table B.2: Finite-sample size and power (%) of other tests under Gaussian noise

Nominal size: 5%											
	Int. (sec)	N_{spl}	BNS	ABD	JO	LM	ASJ	CPR	PZ	MinRV	MedRV
Panel A No Jump	5	4680	0.23	20.28	1.06	14.02	100.00	0.37	5.59	0.00	0.00
	15	1560	4.93	26.64	3.70	22.26	93.73	5.43	9.91	0.91	2.89
	30	780	7.88	26.93	5.02	29.32	38.68	8.42	12.55	4.04	6.35
	60	390	7.69	23.90	6.23	27.86	13.10	8.26	14.47	5.37	7.14
	120	195	7.49	20.82	8.07	17.76	7.10	8.02	16.23	5.71	7.93
	180	130	7.91	18.97	9.05	15.11	5.36	8.70	16.12	5.78	8.78
	300	78	7.74	15.54	10.98	11.96	4.22	8.70	14.91	5.67	9.12
Panel B Moderate Jump	5	4680	44.28	76.55	51.82	69.09	99.76	47.13	66.49	40.11	45.46
	15	1560	40.43	73.96	44.90	60.35	92.97	43.88	61.13	37.19	41.85
	30	780	36.17	68.73	38.30	51.11	65.25	39.14	52.79	33.48	36.97
	60	390	29.52	60.12	30.92	42.23	37.60	32.97	43.63	27.36	31.32
	120	195	21.55	50.01	22.20	36.06	22.08	24.92	32.72	21.00	24.32
	180	130	17.48	42.85	17.40	30.52	14.55	20.17	26.98	17.02	20.84
	300	78	15.27	34.45	11.91	21.62	11.67	17.54	19.96	14.36	16.51
Panel C Large Jump	5	4680	68.50	87.98	74.10	84.55	99.83	70.65	82.69	64.96	68.91
	15	1560	65.66	86.64	69.37	79.03	95.72	68.29	79.36	62.52	66.47
	30	780	61.28	83.55	64.47	73.60	78.16	64.28	74.79	58.50	62.36
	60	390	55.16	79.09	57.63	67.45	57.04	58.50	68.70	52.97	57.53
	120	195	46.02	71.16	48.22	61.94	36.07	50.16	59.34	44.72	49.98
	180	130	41.61	65.42	42.27	56.76	26.63	45.35	53.82	40.37	44.59
	300	78	35.12	57.46	33.77	46.86	17.83	39.24	45.27	34.30	38.21

This table reports the finite-sample size and size-adjusted power (%) of 10,000 simulations of 9 classical tests at 5% nominal level: BNS (Barndorff-Nielsen and Shephard, 2006), ABD (Andersen et al., 2007b), JO (Jiang and Oomen, 2008), LM (Lee and Mykland, 2008), ASJ (Aït-Sahalia and Jacod, 2009), CPR (Corsi et al., 2010), PZ (Podolskij and Ziggel, 2010), MinRV and MedRV (Andersen et al., 2012). All these tests are constructed on observations equidistantly sampled with various intervals in calendar time: 5, 15, 30, 60, 120, 180 and 300 seconds, and "N_{spl}" stands for the sampling frequencies.

Table B.3: Finite-sample size and power (%) of other noise-robust tests under Gaussian noise

Nominal size: 5%					
	Int. (sec)	N_{spl}	PZ*	LM12	ASJL
No Jump	tick	23400	5.10	3.27	5.12
	5	4680	4.93	8.59	8.79
Moderate Jump	tick	23400	39.34	24.12	38.06
	5	4680	29.96	18.97	16.88
Large Jump	tick	23400	64.18	39.18	62.90
	5	7680	56.03	32.23	41.41

This table reports the finite-sample size and size-adjusted power (%) of 10,000 simulations of 3 noise-robust tests at 5% nominal level: noise-adjusted PZ (Podolskij and Ziggel, 2010), LM12 (Lee and Mykland, 2012), and ASJL (Aït-Sahalia et al., 2012). All these tests are constructed on tick-level and 5-second-sampled observations. The tuning parameters for those tests are selected by minimizing the absolute distance between the nominal size and the empirical size with the simulated tick-level noise-contaminated observations.

Table B.4: Finite-sample size and power (%) under autocorrelated Gaussian noise

Nominal size: 5%		$\theta = 0.3$				$\theta = 0.4$				$\theta = 0.5$			
			ϵ				ϵ				ϵ		
	$c/\sigma(\tilde{r}_i)$	$N^{(c)}$	0.05	0.07	0.10	$N^{(c)}$	0.05	0.07	0.10	$N^{(c)}$	0.05	0.07	0.10
Panel A No Jump	3	1785	4.85	5.28	5.39	1784	5.14	5.34	5.69	1783	5.38	5.70	5.84
	4	1099	5.02	5.36	5.34	1099	5.05	4.94	5.32	1097	5.23	5.62	5.69
	5	743	4.84	5.45	4.96	743	4.82	5.58	5.37	743	5.41	5.64	6.07
	6	536	4.71	5.14	5.30	536	4.87	5.32	5.23	535	4.73	5.33	5.63
	7	404	5.21	5.36	5.44	404	5.11	4.91	5.60	404	5.20	5.02	5.45
	8	316	4.74	5.21	5.50	316	4.91	4.79	5.74	316	4.75	5.17	5.41
	9	253	4.56	5.05	5.37	254	4.92	5.16	5.35	253	4.86	5.36	5.32
	10	208	4.87	5.45	5.33	208	5.01	5.48	5.77	208	5.36	5.42	5.75
Panel B Moderate Jump	3	1715	47.02	49.41	52.39	1717	45.14	47.22	49.69	1719	43.27	45.53	48.29
	4	1058	46.22	48.63	51.34	1059	43.97	46.88	48.80	1061	42.70	44.28	47.16
	5	717	45.80	47.83	51.35	719	43.38	45.64	48.35	720	40.70	43.64	45.82
	6	518	45.25	46.85	49.59	519	41.62	45.13	47.71	520	40.83	42.25	45.93
	7	392	43.53	46.57	48.48	393	41.06	44.33	46.80	394	39.47	42.48	45.30
	8	307	43.39	45.85	49.41	308	41.95	43.80	46.44	309	39.25	41.64	44.64
	9	247	43.28	45.83	48.46	248	40.78	43.20	46.57	248	39.04	40.64	45.10
	10	203	42.70	44.97	48.27	204	40.26	41.86	45.96	204	38.51	40.48	43.28
Panel C Large Jump	3	1587	69.39	70.70	72.91	1590	67.87	69.33	71.27	1594	66.82	68.17	70.24
	4	979	68.87	70.46	72.68	983	66.80	69.17	70.63	985	65.84	67.74	69.17
	5	665	67.98	70.11	72.16	668	66.93	68.16	70.27	671	65.21	66.26	68.55
	6	482	68.20	69.38	71.78	485	65.87	67.95	69.81	487	64.66	66.04	67.63
	7	366	66.57	68.81	71.08	368	65.20	67.12	68.95	370	64.53	66.31	67.93
	8	287	67.04	69.14	71.08	289	64.39	66.85	69.28	291	63.97	65.09	67.34
	9	232	66.01	68.47	70.40	234	64.17	66.33	69.04	235	63.15	64.93	67.69
	10	191	66.15	67.95	70.27	193	63.67	65.80	68.23	194	62.39	64.69	67.11

This table reports the finite-sample size and size-adjusted power (%) of 10,000 simulations of the test statistic $T_{c,\epsilon}$ at 5% nominal level. All simulated prices are contaminated by the additive autocorrelated Gaussian noise and rounding errors. We utilize the two-step noise reduction method in Section 3.2 to construct the sequence of pseudo-observations with three different pre-averaging windows, i.e., $k_n = \lceil \theta\sqrt{N} \rceil$ with $\theta \in \{0.3, 0.4, 0.5\}$. The observations are sampled with different PDS barrier widths $c = K\sigma(\tilde{r}_i)$, where K ranges from 3 to 10. Different censoring thresholds with $\epsilon \in \{0.05, 0.07, 0.1\}$ are considered. $N^{(c)}$ stands for the average sampling frequencies.

Table B.5: Finite-sample size and power (%) of other tests under autocorrelated Gaussian noise

Nominal size: 5%											
	Int. (sec)	N_{spl}	BNS	ABD	JO	LM	ASJ	CPR	PZ	MinRV	MedRV
Panel A No Jump	5	4680	0.00	15.38	0.72	10.46	100.00	0.00	5.19	0.00	0.00
	15	1560	2.48	22.98	2.79	19.26	97.34	2.84	8.11	0.40	1.59
	30	780	5.59	24.77	4.27	26.71	47.36	6.32	11.46	2.93	4.99
	60	390	6.84	23.25	5.87	26.53	14.89	7.32	13.67	4.93	6.60
	120	195	7.08	20.54	7.43	17.00	8.51	7.64	15.53	5.55	7.50
	180	130	7.33	17.86	8.53	14.31	5.60	8.09	15.63	5.56	7.98
	300	78	7.92	15.88	10.90	12.15	4.35	9.20	15.09	5.73	9.55
Panel B Moderate Jump	5	4680	42.34	73.62	49.60	68.05	99.81	45.64	64.41	37.27	42.66
	15	1560	39.11	71.47	43.61	59.86	93.84	42.79	60.18	36.30	40.82
	30	780	36.35	66.97	37.43	50.10	66.10	40.00	52.66	32.51	37.08
	60	390	28.49	59.32	29.46	41.52	39.38	32.06	43.30	26.18	30.62
	120	195	22.16	48.88	21.09	34.90	21.09	25.48	32.18	20.48	23.39
	180	130	17.80	41.66	16.58	29.83	15.66	20.78	25.61	17.18	19.83
	300	78	13.36	32.57	11.19	19.64	10.68	14.91	18.07	12.98	14.99
Panel C Large Jump	5	4680	66.02	86.02	71.75	83.05	99.73	68.49	80.74	61.79	66.31
	15	1560	63.75	85.06	67.48	78.59	95.40	66.49	78.52	61.00	64.90
	30	780	60.36	82.44	62.07	72.40	78.66	63.52	73.58	57.06	61.05
	60	390	53.77	76.70	55.08	65.78	56.45	57.05	67.04	51.59	55.26
	120	195	46.55	68.90	46.82	60.23	35.58	49.80	57.96	44.44	48.75
	180	130	40.73	64.47	41.31	55.31	24.87	44.99	51.75	39.56	44.64
	300	78	33.58	56.01	32.74	44.99	16.57	37.28	42.89	32.71	36.46

This table reports the finite-sample size and size-adjusted power (%) of 10,000 simulations of 9 classical tests at 5% nominal level: BNS (Barndorff-Nielsen and Shephard, 2006), ABD (Andersen et al., 2007b), JO (Jiang and Oomen, 2008), LM (Lee and Mykland, 2008), ASJ (Aït-Sahalia and Jacod, 2009), CPR (Corsi et al., 2010), PZ (Podolskij and Ziggel, 2010), MinRV and MedRV (Andersen et al., 2012). All these tests are constructed on observations equidistantly sampled with various intervals in calendar time: 5, 15, 30, 60, 120, 180 and 300 seconds, and "N_{spl}" stands for the sampling frequencies.

Table B.6: Finite-sample size and power (%) of other noise-robust tests under autocorrelated Gaussian noise

Nominal size: 5%					
	Int. (sec)	N_{spl}	PZ*	LM12	ASJL
No Jump	tick	23400	5.06	2.91	5.19
	5	4680	4.98	8.10	8.92
Moderate Jump	tick	23400	38.51	21.87	37.46
	5	4680	29.10	18.91	17.09
Large Jump	tick	23400	65.58	39.64	63.69
	5	7680	55.98	32.62	41.88

This table reports the finite-sample size and size-adjusted power (%) of 10,000 simulations of 3 noise-robust tests at 5% nominal level: noise-adjusted PZ (Podolskij and Ziggel, 2010), LM12 (Lee and Mykland, 2012), and ASJL (Aït-Sahalia et al., 2012). All these tests are constructed on tick-level and 5-second-sampled observations. The tuning parameters for those tests are selected by minimizing the absolute distance between the nominal size and the empirical size with the simulated tick-level noise-contaminated observations.

Table B.7: Finite-sample size and power (%) under t-distributed noise

Nominal size: 5%		$\theta = 0.3$				$\theta = 0.4$				$\theta = 0.5$			
			ϵ				ϵ				ϵ		
	$c/\sigma(\tilde{r}_i)$	$N^{(c)}$	0.05	0.07	0.10	$N^{(c)}$	0.05	0.07	0.10	$N^{(c)}$	0.05	0.07	0.10
Panel A No Jump	3	1785	4.74	5.28	5.54	1784	5.25	5.01	5.79	1783	5.04	5.38	5.73
	4	1100	5.01	5.04	5.40	1098	5.05	5.00	5.78	1098	5.05	5.10	5.61
	5	743	4.62	4.85	5.29	743	4.77	5.04	5.51	743	4.60	5.31	5.82
	6	536	4.93	5.01	5.35	535	4.67	5.01	5.42	535	4.81	5.44	5.81
	7	404	4.83	5.08	5.22	404	4.81	5.04	5.48	403	5.24	5.58	5.67
	8	316	4.86	5.34	5.27	316	4.91	5.22	5.67	316	4.88	5.15	5.70
	9	254	4.77	5.42	5.24	253	5.13	5.41	5.39	253	4.83	5.01	5.72
	10	208	5.12	5.37	5.64	208	5.27	5.56	5.77	208	4.93	5.62	5.84
Panel B Moderate Jump	3	1716	46.47	48.75	50.70	1718	44.29	46.93	48.39	1718	42.42	45.03	46.94
	4	1058	45.56	48.39	50.84	1060	43.27	45.47	47.73	1061	41.57	43.20	45.28
	5	717	45.09	47.07	50.32	719	42.73	45.48	47.82	720	40.67	42.31	45.21
	6	519	44.78	46.46	48.26	519	41.76	44.18	46.61	521	40.50	42.15	44.40
	7	392	44.00	45.75	48.66	393	40.80	43.60	46.14	394	39.99	41.48	43.88
	8	307	42.56	44.26	48.15	308	40.08	42.59	45.58	308	39.08	41.55	43.25
	9	247	42.79	44.68	48.11	248	39.44	41.88	45.47	248	38.55	41.12	42.51
	10	203	41.21	44.19	46.88	204	39.69	41.62	44.87	204	37.62	39.87	42.92
Panel C Large Jump	3	1585	70.44	71.21	73.23	1589	68.58	70.69	72.01	1592	66.90	68.86	70.80
	4	978	69.91	71.37	73.07	981	68.25	69.64	71.07	985	66.59	68.75	69.66
	5	664	69.36	71.15	72.79	668	67.65	69.30	71.08	670	66.09	67.79	69.56
	6	481	68.75	70.43	72.67	484	66.82	68.64	70.50	487	65.24	66.70	68.72
	7	365	68.08	69.77	71.74	368	65.70	67.87	69.97	370	64.57	66.43	68.83
	8	287	67.67	68.95	70.93	289	65.10	68.12	69.69	291	63.77	66.09	67.83
	9	232	66.89	68.86	71.66	234	64.52	66.96	69.63	235	63.39	66.10	67.81
	10	191	66.21	68.25	70.90	192	64.24	66.28	69.49	194	62.52	64.96	67.43

This table reports the finite-sample size and size-adjusted power (%) of 10,000 simulations of the test statistic $T_{c,\epsilon}$ at 5% nominal level. All simulated prices are contaminated by the additive t-distributed noise and rounding errors. We utilize the two-step noise reduction method in Section 3.2 to construct the sequence of pseudo-observations with three different pre-averaging windows, i.e., $k_n = \lceil \theta\sqrt{N} \rceil$ with $\theta \in \{0.3, 0.4, 0.5\}$. The observations are sampled with different PDS barrier widths $c = K\sigma(\tilde{r}_i)$, where K ranges from 3 to 10. Different censoring thresholds with $\epsilon \in \{0.05, 0.07, 0.1\}$ are considered. $N^{(c)}$ stands for the average sampling frequencies.

Table B.8: Finite-sample size and power (%) of other tests under t-distributed noise

	Int. (sec)	N_{spl}	BNS	ABD	JO	LM	ASJ	CPR	PZ	MinRV	MedRV
Panel A No Jump	5	4680	58.90	100.00	15.85	100.00	99.92	99.87	99.70	0.12	0.02
	15	1560	12.76	90.37	10.10	89.87	92.05	56.23	72.27	0.71	2.19
	30	780	8.89	59.49	7.81	62.42	44.91	24.70	40.96	3.06	5.18
	60	390	7.25	35.24	7.38	38.66	16.35	11.91	24.07	4.49	7.09
	120	195	7.23	23.72	8.22	20.16	7.68	8.87	18.31	5.11	7.38
	180	130	7.37	19.82	8.99	16.35	5.38	8.42	17.48	5.30	8.46
	300	78	7.34	15.19	10.83	11.47	4.33	8.64	14.86	5.22	8.55
Panel B Moderate Jump	5	4680	37.49	100.00	37.05	17.64	99.97	11.25	13.71	39.54	41.12
	15	1560	40.61	96.71	38.20	25.74	97.85	21.65	20.95	34.45	37.18
	30	780	36.25	82.85	35.77	31.96	70.97	30.82	27.51	31.47	35.67
	60	390	30.11	65.91	29.45	36.41	40.48	30.72	35.36	27.12	31.05
	120	195	22.54	50.98	21.73	34.11	21.92	24.58	30.89	20.59	23.94
	180	130	17.55	43.33	17.67	29.39	14.43	20.16	25.77	16.98	20.66
	300	78	14.49	34.14	12.22	22.25	10.45	16.11	20.07	13.74	17.01
Panel C Large Jump	5	4680	62.75	100.00	63.82	45.20	99.98	31.59	38.22	63.94	65.60
	15	1560	65.71	98.39	64.24	53.45	98.79	47.84	47.73	59.14	61.94
	30	780	61.92	91.00	62.02	59.38	81.94	56.98	54.91	56.36	60.86
	60	390	55.55	82.02	55.88	63.00	57.74	56.36	62.26	52.38	56.60
	120	195	47.62	71.89	47.85	60.48	37.89	51.29	57.77	45.42	50.37
	180	130	41.65	65.87	43.02	55.53	25.61	45.02	52.02	40.67	45.06
	300	78	35.10	57.50	34.13	47.57	16.34	39.19	45.37	34.32	39.24

This table reports the finite-sample size and size-adjusted power (%) of 10,000 simulations of 9 classical tests at 5% nominal level: BNS (Barndorff-Nielsen and Shephard, 2006), ABD (Andersen et al., 2007b), JO (Jiang and Oomen, 2008), LM (Lee and Mykland, 2008), ASJ (Aït-Sahalia and Jacod, 2009), CPR (Corsi et al., 2010), PZ (Podolskij and Ziggel, 2010), MinRV and MedRV (Andersen et al., 2012). All these tests are constructed on observations equidistantly sampled with various intervals in calendar time: 5, 15, 30, 60, 120, 180 and 300 seconds, and "N_{spl}" stands for the sampling frequencies.

Table B.9: Finite-sample size and power (%) of other noise-robust tests under t-distributed noise

Nominal size: 5%					
	Int. (sec)	N_{spl}	PZ*	LM12	ASJL
No Jump	tick	23400	5.07	5.46	6.18
	5	4680	4.64	9.24	8.74
Moderate Jump	tick	23400	39.40	25.31	37.68
	5	4680	29.26	18.76	17.19
Large Jump	tick	23400	65.11	41.81	62.48
	5	7680	55.60	31.85	41.42

This table reports the finite-sample size and size-adjusted power (%) of 10,000 simulations of 3 noise-robust tests at 5% nominal level: noise-adjusted PZ (Podolskij and Ziggel, 2010), LM12 (Lee and Mykland, 2012), and ASJL (Aït-Sahalia et al., 2012). All these tests are constructed on tick-level and 5-second-sampled observations. The tuning parameters for those tests are selected by minimizing the absolute distance between the nominal size and the empirical size with the simulated tick-level noise-contaminated observations.

B.3 Supplementary Empirical Results

Table B.10 reports the empirical results for 7 other tests. Based on the simulation results in Tables 3 and 4, we select four calendar-time-sampling-based tests: BNS, CPR, MinRV and MedRV, with different sampling intervals: 30, 60, 120, and 300 seconds, and we also construct the noise-robust tests PZ*, LM12 and ASJL from tick-by-tick and 5-second data. For most of the selected stocks, the noise-robust ASJL constructed from tick-level observations obtains comparable results to our PDS-based test.

Table B.10: Empirical rejection rates (%) of other tests for selected NYSE stocks

Test	Int. (sec)	AXP	BA	DIS	IBM	JNJ	JPM	MRK	MCD	PG	WMT
BNS	30	32.02	20.55	20.95	28.46	36.36	32.81	49.80	25.69	43.08	32.41
	60	20.16	11.07	19.37	25.69	28.06	24.51	37.55	26.09	31.23	26.88
	120	17.00	16.21	16.21	22.53	27.67	25.30	25.69	23.32	27.27	27.67
	300	18.58	18.58	15.42	19.76	20.16	17.00	23.32	22.13	22.13	22.13
CPR	30	38.34	32.02	35.57	39.13	47.83	38.34	59.29	33.20	52.57	41.11
	60	28.46	16.60	26.88	33.99	40.32	32.41	45.85	29.25	40.32	35.57
	120	25.30	20.16	21.74	30.83	34.78	32.02	33.99	28.85	32.81	33.60
	300	23.32	23.72	21.34	27.67	29.64	22.13	32.81	28.46	30.43	30.83
MinRV	30	22.53	17.39	15.42	18.18	22.92	21.74	27.67	19.76	26.48	21.34
	60	14.23	9.88	15.42	19.76	21.74	16.21	22.92	20.95	22.13	22.13
	120	14.23	12.65	12.65	18.58	18.18	17.79	18.58	19.76	19.76	21.74
	300	13.04	14.62	13.83	17.39	13.04	11.07	15.81	15.42	16.21	14.23
MedRV	30	30.83	23.72	28.46	31.62	37.15	29.64	40.71	29.64	37.94	32.02
	60	20.55	15.81	22.92	28.46	37.15	27.67	33.60	28.85	32.81	30.04
	120	20.55	18.58	18.58	26.48	29.64	26.48	27.27	26.88	28.85	34.78
	300	18.97	17.00	16.60	24.11	21.74	20.55	23.72	24.90	28.06	25.30
PZ*	tick	7.51	6.32	6.32	5.93	6.32	6.72	7.51	5.14	7.51	4.74
	5	31.23	22.92	19.76	26.09	22.13	23.32	23.72	24.90	30.04	31.62
LM12	tick	12.65	4.35	7.51	9.49	12.65	11.46	12.65	9.49	18.58	11.86
	5	32.02	21.34	30.04	37.55	29.25	27.27	38.74	27.67	40.32	35.18
ASJL	tick	15.81	20.16	13.04	13.83	13.83	13.44	15.02	20.55	13.83	15.02
	5	32.02	20.95	29.25	21.34	26.48	21.74	22.92	26.09	30.04	32.41

This table reports the proportions of days with jumps for 10 NYSE stocks in 2020, as identified by the following procedures: BNS (Barndorff-Nielsen and Shephard, 2006), CPR (Corsi et al., 2010), PZ (Podolskij and Ziggel, 2010), MinRV and MedRV (Andersen et al., 2012), PZ* (Podolskij and Ziggel, 2010), LM12 (Lee and Mykland, 2012), and ASJL (Aït-Sahalia et al., 2012). The first 4 tests are constructed from observations equidistantly sampled in calendar time (with the last tick interpolation): 30, 60, 120 and 300 seconds. The noise-adjusted PZ*, LM12, and ASJL are constructed from tick-by-tick and 5-second-sampled data. The total number of trading days is 253.

Table B.11 reports the empirical results for other tests constructed from calendar-time-sampled data, with the control of spurious detections using the thresholding methods in Bajgrowicz et al. (2016): (i) the universal threshold $\sqrt{2\ln 253}$, and (ii) the FDR threshold. We only consider one-sided tests whose limiting distribution is $\mathcal{N}(0,1)$ under the null, which includes the upper-tailed BNS, CPR, MinRV, MedRV, PZ*, and the lower-tailed ASJL, but excludes the Gumbel-distributed LM12.

Table B.11: Adjusted empirical rejection rate (%) of other tests for selected NYSE stocks

	Test	Int. (sec)	AXP	BA	DIS	IBM	JNJ	JPM	MRK	MCD	PG	WMT
Panel A Universal threshold	BNS	30	24.11	18.18	17.79	23.32	27.67	25.69	33.99	20.95	30.83	22.92
		60	15.81	9.09	15.42	19.37	18.58	18.97	29.25	20.55	24.11	20.16
		120	13.44	13.83	15.02	20.55	22.92	22.13	21.74	17.79	19.37	20.55
		300	15.02	16.21	13.04	15.42	16.21	14.62	19.76	17.79	17.00	20.55
	CPR	30	27.67	27.27	29.64	27.67	31.23	26.88	36.76	23.32	33.99	26.48
		60	22.92	13.83	20.55	25.69	27.67	22.92	31.23	20.95	27.67	24.11
		120	21.34	17.00	19.76	24.90	24.11	27.27	25.69	23.32	23.72	24.51
		300	18.18	20.55	16.60	22.53	23.72	18.18	25.69	22.13	21.74	26.09
	MinRV	30	17.79	16.21	13.44	16.21	19.37	18.18	23.32	16.60	20.55	16.60
		60	11.86	8.30	14.23	15.81	17.79	14.62	20.55	18.97	20.16	18.97
		120	12.25	12.25	12.25	18.18	17.39	17.39	15.02	17.79	16.21	18.97
		300	12.25	13.44	13.44	16.21	12.25	11.07	15.42	13.44	15.02	13.83
	MedRV	30	24.51	21.74	26.09	25.30	26.09	21.74	30.04	22.92	28.46	26.09
		60	17.00	14.23	19.76	23.32	29.64	21.34	24.90	25.69	24.11	22.53
		120	17.39	16.21	17.39	21.34	24.11	24.11	22.53	22.13	22.13	29.64
		300	16.21	15.42	15.02	20.55	18.97	18.97	18.18	20.95	24.51	22.13
	PZ*	tick	5.53	5.53	6.32	3.56	3.56	5.93	5.93	3.95	5.14	3.16
		5	2.77	4.35	1.58	3.95	3.16	2.77	2.77	3.16	3.56	4.74
	ASJL	tick	14.23	18.58	13.04	13.04	13.44	12.25	12.25	19.37	13.44	14.62
		5	26.09	17.39	26.09	18.18	21.34	17.00	18.58	22.53	25.30	24.11
Panel B FDR threshold	BNS	30	14.23	15.02	16.21	14.23	12.25	15.02	9.09	14.62	11.46	11.07
		60	13.04	7.11	12.25	12.65	10.28	14.23	15.02	13.04	14.23	9.09
		120	9.88	13.44	14.62	14.62	13.83	17.39	12.25	15.02	13.83	10.28
		300	13.04	13.04	9.88	12.25	13.83	11.46	12.65	13.44	9.09	16.21
	CPR	30	9.09	15.42	19.37	13.04	11.86	9.09	7.51	12.25	8.30	10.28
		60	14.62	10.67	15.02	15.02	13.04	15.02	12.25	11.46	11.07	9.88
		120	13.83	16.21	16.21	13.04	14.62	16.21	13.04	13.44	13.04	10.67
		300	13.04	16.21	11.46	17.00	13.04	10.28	17.79	15.02	13.44	15.42
	MinRV	30	15.81	14.23	12.65	16.21	12.65	17.39	11.07	14.23	15.02	13.83
		60	10.67	7.51	11.07	12.65	12.65	11.86	13.44	18.58	13.44	14.62
		120	10.67	12.25	12.65	18.18	13.83	16.21	14.23	16.21	14.62	16.21
		300	12.65	11.86	13.44	15.81	12.25	11.07	13.04	13.44	15.02	13.83
	MedRV	30	15.02	19.37	19.76	10.28	16.60	16.60	10.67	16.21	17.39	13.44
		60	13.04	13.04	13.44	11.86	19.76	13.04	13.83	18.18	16.60	11.07
		120	15.42	15.02	13.83	15.42	18.58	21.74	16.21	18.97	12.25	18.58
		300	11.07	13.83	9.49	16.60	13.83	16.60	13.04	13.04	16.60	18.97
	PZ*	tick	5.53	5.53	6.32	3.56	3.56	5.93	5.93	3.95	5.14	3.16
		5	2.77	4.35	1.58	3.95	3.16	2.77	2.77	3.16	3.56	4.74
	ASJL	tick	13.04	16.21	13.04	10.28	13.44	12.25	11.07	17.39	13.44	14.62
		5	15.02	13.44	18.58	15.42	15.42	14.23	12.65	18.58	17.39	14.62

This table reports the proportions of days with jumps for 10 NYSE stocks in 2020, as identified by the following procedures: BNS (Barndorff-Nielsen and Shephard, 2006), CPR (Corsi et al., 2010), PZ (Podolskij and Ziggel, 2010), MinRV and MedRV (Andersen et al., 2012), PZ* (Podolskij and Ziggel, 2010), and ASJL (Aït-Sahalia et al., 2012), with the control of spurious detections using the thresholding methods in Bajgrowicz et al. (2016). The first 4 tests are constructed from observations equidistantly sampled in calendar time (with the last tick interpolation): 30, 60, 120 and 300 seconds. The noise-adjusted PZ* and ASJL are constructed from tick-by-tick and 5-second-sampled data. The total number of trading days is 253.